



# Dynamic load of timber truck

TME180 Automotive Engineering Project 2025

RAMKUMAR HULEPPA MUNAVALLI  
VIKTOR LARSSON ROSÉN  
ROHAN KUMAAR VASUDEVAN  
BOXUAN WU

*Department of Mechanics and Maritime Sciences*  
CHALMERS UNIVERSITY OF TECHNOLOGY  
Göteborg, Sweden, 2025

# **Dynamic load of timber truck**

## **TME180 Automotive Engineering Project 2025**

© RAMKUMAR HULEPPA MUNAVALLI, VIKTOR LARSSON  
ROSÉN, ROHAN KUMAAR VASUDEVAN, BOXUAN WU, 2025

Supervisor: Fredrik Bruzelius, Mechanics and Maritime Sciences  
Supervisor: Lennart Cider, Volvo Technology  
Examiner: Alexey Vdovin, Mechanics and Maritime Sciences

Studentarbeten – Mekanik och maritima vetenskaper (M2) – Projektarbete  
Department of Mechanics and Maritime Sciences  
Chalmers University of Technology  
SE-412 96 Göteborg  
Sweden  
Telephone +46 (0)31 772 1000

# Abstract

This project investigates the dynamic load generated by heavy timber truck combination as part of a collaborative research effort between Chalmers university of Technology, NTNU and Volvo Trucks. The overarching goal of the research is to improve the understanding of how trucks and their loads influence bridge structure, with the long term objective of enabling safe reclassification of existing Swedish bridge to higher load limits (BK4).

In this project, the focus is on developing a simplified yet representative dynamics model of a timber truck combination that can later be used for studying Dynamic Amplification Factor (DAF) and truck-bridge interaction. The part involved deriving the equation of motion for the truck and trailer, identifying and estimating key model parameters, and implementing the model in a suitable simulation environment. Parametric studies were carried out to analyze how factors such as road surface irregularities, vehicle speed, suspension characteristic and axle configuration affect the resulting dynamic loads.

Furthermore, the project included the planning and preparation of experimental test using an instrumented timber truck for future model validation. The developed model and proposed testing methodology together provide a foundation for accurately simulating the dynamic behaviour of heavy vehicle and for supporting future studies on the interaction between vehicle and bridges.

## Keywords

Heavy vehicle dynamics, Dynamic vehicle loading, Dynamic amplification factor, Gross vehicle weight, Timber truck, Bridge load assessment.



# Acknowledgements

The authors would like to thank Professor and supervisor Fredrik Bruzelius at Chalmers University of Technology for his guidance, expertise, and continuous support throughout this project. His feedback was essential to the development and quality of the work.

The authors also acknowledge the contributions of Viktor Eriksson (Chalmers), Lennart Cider (Volvo Trucks), and Christoffer Svedholm for their valuable input and feedback. Further thanks are extended to the examiner Alexey Vdovin (Chalmers University of Technology).

This project was conducted as part of the course *Automotive Engineering Project 2025* (TME180) at Chalmers University of Technology.

# Preface

This report presents the results of a student project carried out within the course *Automotive Engineering Project 2025* (TME180) at Chalmers University of Technology. The work was conducted in collaboration with Volvo Trucks and forms part of a broader research initiative focused on heavy vehicle dynamics and bridge load assessment.

The project focuses on the development of a simplified dynamic model of a heavy timber truck and trailer combination. The model is intended to support future studies of vehicle–bridge interaction by providing a transparent and analytically tractable representation of vehicle dynamics. Emphasis is placed on model clarity, parameter transparency, and relevance for bridge load analysis rather than high-fidelity commercial simulation.

The report documents the modelling approach, parameter selection, and validation strategy adopted during the project. The work is intended to serve both as a foundation for continued research within the larger collaboration and as an educational exercise in applied vehicle dynamics and modelling.

# Contents

<b>Acknowledgements</b>	<b>v</b>
<b>Preface</b>	<b>vi</b>
<b>Nomenclature</b>	<b>ix</b>
<b>Abbreviations</b>	<b>xi</b>
<b>1 Introduction</b>	<b>1</b>
1.1 Background and motivation of study . . . . .	1
1.2 Problem statement . . . . .	1
1.3 Problem solving strategy . . . . .	2
1.4 Outline of the report . . . . .	2
<b>2 Theory &amp; Methodology</b>	<b>4</b>
2.1 Theory . . . . .	4
2.2 Methodology . . . . .	4
2.2.1 Modeling . . . . .	4
2.2.2 Parameterization . . . . .	4
2.2.3 Model Analysis . . . . .	5
2.2.4 Testing & Validation . . . . .	5
<b>3 Modelling &amp; Simulations</b>	<b>6</b>
3.1 Variables & Parameters . . . . .	6
3.2 Equations of Motion . . . . .	8
3.3 State-space form . . . . .	9
3.4 Simulink Implementation . . . . .	9
3.5 Experiments . . . . .	9
3.5.1 TruckMaker Simulations . . . . .	9
3.5.2 Simulink Simulations . . . . .	10
3.5.3 Road profile . . . . .	10
3.5.4 Load and Velocity Sweep . . . . .	10
<b>4 Results</b>	<b>11</b>
4.1 Overview . . . . .	11
4.2 Simulations . . . . .	11
4.2.1 Simulation Setup . . . . .	11
4.2.2 Time-Domain Responses . . . . .	12
4.3 Model Validation . . . . .	12
4.4 Load and Velocity Sweep Results . . . . .	13
4.4.1 Effect of Load . . . . .	15
4.4.2 Effect of Velocity . . . . .	17
4.5 Dynamic Amplification Factor (DAF) . . . . .	19
4.6 Summary of Key Findings . . . . .	20
<b>5 Discussion</b>	<b>21</b>
5.1 Interpretation of Model Behaviour . . . . .	21
5.2 Comparison with TruckMaker . . . . .	21
5.3 Influence of Load and Velocity . . . . .	22
5.4 Limitations of the Model . . . . .	22

5.5	Reliability and Applicability of the Results . . . . .	23
<b>6</b>	<b>Conclusions</b>	<b>24</b>
<b>7</b>	<b>Future work</b>	<b>25</b>
	<b>References</b>	<b>26</b>
	<b>Appendices</b>	<b>I</b>
<b>A</b>	<b>Parameter list</b>	<b>I</b>
<b>B</b>	<b>State-Space model</b>	<b>III</b>
B.1	Equations of Motion . . . . .	III
B.1.1	Sprung Mass (Truck and Trailer) . . . . .	III
B.1.2	Un-sprung Masses (Truck and Trailer) . . . . .	III
B.1.3	Drawbar Dynamics . . . . .	IV
B.2	Matlab script . . . . .	V
<b>C</b>	<b>Simulink model</b>	<b>XXI</b>
C.1	CASE – 1: Speed Bump . . . . .	XXI
C.2	CASE – 2: Road & Bridge Expansion Joint . . . . .	XXI
<b>D</b>	<b>Load and Velocity Sweep</b>	<b>XXII</b>
D.1	CASE – 1: Speed Bump . . . . .	XXII
D.2	CASE – 2: Road & Bridge Expansion Joint . . . . .	XXVIII

# Nomenclature

Symbol	Description
$y$	Vertical displacement (heave) of the truck chassis [m]
$\phi_1$	Pitch angle of the truck body [rad]
$\dot{y}$	Rate of change of Vertical displacement (heave) of the truck [m/s]
$\dot{\phi}_1$	Rate of change of Pitch angle of the truck [rad/s]
$Y$	Vertical displacement (heave) of the trailer chassis [m]
$\phi_2$	Pitch angle of the trailer body [rad]
$\dot{Y}$	Rate of change of Vertical displacement (heave) of the trailer [m/s]
$\dot{\phi}_2$	Rate of change of Pitch angle of the trailer body [rad/s]
$w$	Vertical displacement (heave) of the drawbar [m]
$\phi_3$	Pitch angle of the drawbar [rad]
$\dot{w}$	Rate of change of Vertical displacement (heave) of the drawbar [m/s]
$\dot{\phi}_3$	Rate of change of Pitch angle of the drawbar [rad/s]
$y_1$	Vertical displacement (heave) of front axle group of the truck [m]
$y_2$	Vertical displacement (heave) of rear axle group of the truck [m]
$y_3$	Vertical displacement (heave) of front axle group of the trailer [m]
$y_4$	Vertical displacement (heave) of rear axle group of the trailer [m]
$\dot{y}_1$	Rate of change of Vertical displacement of front axle group of the truck [m/s]
$\dot{y}_2$	Rate of change of Vertical displacement of rear axle group of the truck [m/s]
$\dot{y}_3$	Rate of change of Vertical displacement of front axle group of the trailer [m/s]
$\dot{y}_4$	Rate of change of Vertical displacement of rear axle group of the trailer [m/s]
$C_{sf}, D_{sf}$	Truck front suspension stiffness and damping coefficient [N/m, Ns/m]
$C_{sr}, D_{sr}$	Truck rear suspension stiffness and damping coefficient [N/m, Ns/m]
$C_{sft}, D_{sft}$	Trailer front suspension stiffness and damping coefficient [N/m, Ns/m]
$C_{srt}, D_{srt}$	Trailer rear suspension stiffness and damping coefficient [N/m, Ns/m]
$C_{wf}, D_{wf}$	Truck front tire radial stiffness and damping coefficient [N/m, Ns/m]
$C_{wr}, D_{wr}$	Truck rear tire radial stiffness and damping coefficient [N/m, Ns/m]
$C_{wtf}, D_{wtf}$	Trailer front tire radial stiffness and damping coefficient [N/m, Ns/m]

$C_{wtr}, D_{wtr}$	Trailer rear tire radial stiffness and damping coefficient [N/m, Ns/m]
$C_{sd}, D_{sd}$	Drawbar spring stiffness and damping coefficient [N/m, Ns/m]
$l_f, l_r$	Distance from CoG to truck's front and rear axle group [m]
$l_{ft}, l_{rt}$	Distance from CoG to trailer's front and rear axle group [m]
$l_{fd}, l_{rd}$	Distance from drawbar's CoG to truck's front and rear articulation point [m]
$a_1$	Distance from truck's CoG to drawbar front articulation point [m]
$a_2$	Distance from trailer's CoG to drawbar rear articulation point [m]
$m_c$	mass of the truck chassis [sprung] [kg]
$m_{ct}$	mass of the trailer chassis [sprung] [kg]
$m_d$	mass of the drawbar [kg]
$m_{uf}, m_{ur}$	mass of the front and rear axle groups of truck [unsprung] [kg]
$m_{uft}, m_{urt}$	mass of the front and rear axle groups of trailer [unsprung] [kg]
$I_y$	Mass moment of inertia in pitch axis for truck chassis [kg.m <sup>2</sup> ]
$I_{yt}$	Mass moment of inertia in pitch axis for trailer chassis [kg.m <sup>2</sup> ]
$I_{yd}$	Mass moment of inertia in pitch axis for drawbar [kg.m <sup>2</sup> ]
$V_x$	Constant forward velocity [m/s]

## Abbreviations

<b>BK4</b>	Bärighetsklass 4 (Max 74 tons gross weight)
<b>DOF</b>	Degrees of Freedom
<b>LHS</b>	Latin Hypercube Sampling
<b>DAF</b>	Dynamic Amplification Factor
<b>LHS</b>	Latin Hypercube Sampling
<b>r.m.s</b>	Root mean square

# 1 Introduction

## 1.1 Background and motivation of study

Chalmers University of Technology, in collaboration with the Norwegian University of Science and Technology (NTNU) and Volvo Trucks, is currently conducting a research project aimed at investigating the dynamic loads that heavy vehicles exert on bridges. Volvo Trucks contributes as the vehicle representative, while the academic partners provide expertise in vehicle dynamics and structural engineering. Together, the project focuses on understanding the interaction between heavy vehicle dynamics and bridge capacity, with the overarching objective of supporting safer and more efficient use of existing transport infrastructure.

A heavy timber truck combination has been selected as the representative vehicle due to its high load capacity due to the new regulations for the study. This vehicle type is particularly relevant due to its high gross weight and its importance to Swedish industry, especially within the forestry sector. An additional advantage of the timber truck is its operational flexibility, as it can be tested in both loaded and unloaded configurations, enabling a broad investigation of vehicle dynamic behaviour under varying mass conditions.

The broader motivation for the project is linked to the ongoing transition toward heavier and more efficient road transport in Sweden. Industries such as forestry, mining, and construction increasingly depend on high-capacity vehicles to remain competitive. In response, the Swedish road authority introduced the highest load-capacity class, BK4 (Bärighetsklass 4), in 2018. BK4 permits vehicle combinations with a gross weight of up to 74 tons, compared to the standard limit of 64 tons. Despite this regulatory change, the implementation of BK4 remains limited. By the end of 2024, only approximately 66% of Sweden's strategic road network was approved for BK4 traffic, while the national target is to reach 70–80% by 2029 (von Hofsten et al., 2024).

The primary limiting factor for wider BK4 adoption are bridges, as many existing structures have not been approved for higher load classes. In many cases, these bridges may possess sufficient structural capacity to carry BK4 vehicles, but current assessment methods are conservative or lack validation for modern heavy vehicle configurations. As a result, bridges cannot be safely reclassified without improved tools for evaluating the true effects of dynamic vehicle loads (Wik, 2025).

Limited access to BK4-classified roads has several consequences. Transport routes become longer or more restricted, increasing operational costs and reducing logistical efficiency. Furthermore, the environmental benefits associated with BK4 transport are not fully realized. Heavier vehicle combinations can reduce the number of trips required to transport the same amount of goods, leading to lower overall emissions. When access is restricted, these potential climate benefits are lost. Improving the understanding of heavy vehicle–bridge interaction is therefore not only an infrastructure challenge but also an economic and environmental priority.

## 1.2 Problem statement

This project forms part of the initial phase of a larger research effort aimed at improving the assessment of bridge loads induced by heavy vehicles. The objective is to develop a simplified yet comprehensive dynamic model of a heavy timber truck and trailer combination that can serve as a basis for future vehicle–bridge interaction studies.

The model is implemented in a MATLAB and Simulink environment, where the equations of motion are derived explicitly to ensure transparency and full control over system parameters. Vehicle properties such as masses, suspension characteristics, axle configurations, and load distributions are defined so that the model accurately represents the physical timber truck. The simplified modelling approach is chosen to support analytical understanding, facilitate collaboration with bridge engineers, and provide direct access to force quantities relevant for bridge assessment.

Model validation is performed by comparing the simplified model with results from more detailed vehicle dynamics simulation models. Representative excitation cases, such as speed bumps and bridge expansion joints, are used to evaluate the vehicle's dynamic response, with particular emphasis on quantities relevant for bridge loading, including the Dynamic Amplification Factor. Ultimately, the model is intended to support reliable bridge capacity assessments and enable future studies of truck-bridge interaction.

The specific objectives of the project are to:

- Derive the mathematical model describing the vehicle dynamics of the timber truck and trailer combination.
- Identify and estimate the relevant parameters required for accurate representation of the physical vehicle.
- Validate the model using simulation and experimental data obtained from physical testing.

### 1.3 Problem solving strategy

The work in this project is organized into four main work packages (WPs):

- **WP1: Modelling**  
Derive the equations of motion for the truck combination and implement the model in a suitable software environment for subsequent analysis.
- **WP2: Parameterization**  
Identify all parameters relevant to the model that can be determined analytically or through manufacturer data. Propose and plan additional experiments required to obtain parameters that cannot be estimated directly.
- **WP3: Model Analysis**  
Conduct analyses using the developed model to investigate how dynamic loads depend on factors such as road surface irregularities, vehicle speed, suspension characteristics, and axle configuration.
- **WP4: Testing and Validation**  
Perform validation tests with a instrumented timber truck or Truck-Maker simulation software. Compare the measured results with the model outputs to assess the model's accuracy and reliability.

### 1.4 Outline of the report

The report is structured as follows:

- **Chapter 1 – Introduction:** Presents the background, motivation, and problem statement, together with the overall objectives and scope of the study.

- **Chapter 2 – Theory & Methodology:** Describes the theoretical framework, modelling approach, and methodologies applied to analyse and solve the problem.
- **Chapter 3 – Modelling & Simulations:** Details the derivation and implementation of the dynamic model, including parameter identification and simulation setup.
- **Chapter 4 – Results:** Presents the outcomes from the simulations and analyses, highlighting key findings and performance indicators.
- **Chapter 5 – Discussion:** Interprets the obtained results, evaluates model behaviour, and discusses limitations and implications.
- **Chapter 6 – Conclusions:** Summarises the main findings and conclusions drawn from the study in relation to the research objectives.
- **Chapter 7 – Future Work:** Suggests possible improvements, extensions, and directions for continued research and experimental validation.

## 2 Theory & Methodology

### 2.1 Theory

The importance of the vehicle–bridge interaction problem has led to extensive research aimed at understanding the dynamic response of bridges subjected to moving vehicles. Within the broader context of this research area, the long-term objective is to assess the feasibility of upgrading a single-span bridge to BK4 classification, corresponding to a 74-tonne load-carrying capacity, using vehicle-induced dynamic loading effects.

When an heavy truck travels over the bridge, the structural response of the bridge is influenced not only by static loading but also dynamic loading effects. These dynamic effects depend on the vehicle suspension’s characteristics, road surface irregularities, vehicle speed and load. This dynamic component can amplify the effective force transmitted to the bridge, affecting both the fatigue life and load classification. The dynamic amplification factor (DAF) quantifies the structural or load response due to dynamics effect compared to static conditions. Both the bridge and the vehicle are subjected to additional dynamic forces governed by their respective inertial, damping, and stiffness properties.

The scope of the present project is limited to the development of a simplified simulation model of a truck–trailer combination. The model incorporates the full truck–trailer and axle masses, centres of gravity, pitch motion, and rotational inertias, together with suspension and tyre stiffness and damping characteristics. The vehicle is assumed to travel at a constant speed. As the vehicle traverses the bridge under different excitation profiles, the resulting tyre contact forces at the tyre–road interface are computed and analysed.

These tyre contact forces constitute the primary output of this study and will be used in subsequent research to apply moving loads to a bridge model. The modelling of the bridge response and the calculation of the dynamic amplification factor (DAF) are therefore beyond the scope of this report and will be addressed in later stages of the overall research programme.

### 2.2 Methodology

#### 2.2.1 Modeling

Deriving the equation for the truck-trailer combination, solving and implementing the model in the MATLAB and Simulink environment for analysis. The model will focus initially on the vertical, pitch to capture dynamic load variations at the wheel contact patch.

#### 2.2.2 Parameterization

The model parameters are derived from relevant vehicle data and design documentation. These include the vehicle mass, centre of gravity location, and overall geometric dimensions, as well as the stiffness and damping coefficients of the suspension system. In addition, tyre stiffness and damping properties are incorporated to accurately represent tyre–road interactions. Axle spacing and axle load characteristics are also defined to ensure a realistic representation of the vehicle’s load distribution and dynamic behaviour.

Figure 1 illustrates the key truck and trailer parameters considered in the model.

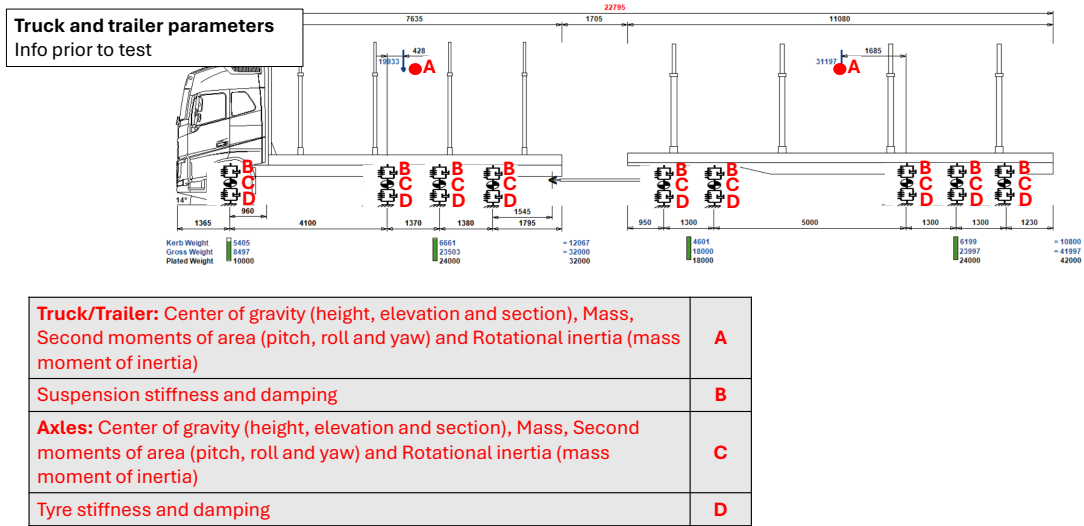


Figure 1: Truck and Trailer parameters

### 2.2.3 Model Analysis

The parameterized model will be analysed to investigate the dependence of dynamic load on vehicle operating conditions. In particular, the effects of vehicle speed and payload are examined under a range of road excitation profiles, allowing the influence of varying road inputs on dynamic load response to be systematically assessed.

### 2.2.4 Testing & Validation

The developed model is validated through comparison with ground truth simulations (scenarios) conducted in IPG TruckMaker. The TruckMaker vehicle model serves as a reference representation of a truck-trailer dynamics, incorporating detailed vehicle, suspension, and tyre characteristics. Key dynamic responses obtained from the proposed model are compared against corresponding TruckMaker simulation outputs under equivalent operating conditions and road excitation profiles.

This simulation-based validation ensures that the model adequately captures the essential dynamic behaviour of the vehicle. Full-scale validation using a real truck-trailer configuration and measurements from a bridge is planned for subsequent project stages beyond the scope of this report. Following these future validation activities, the model will be employed for comprehensive vehicle-bridge interaction analyses in later phases of the project.

### 3 Modelling & Simulations

This section summarizes the modelling choices and how the model is implemented in MATLAB/Simulink. The model was developed with half-car model initially in mind (Mahamdnur, 2019), (Gang Wang, 2016) and expanded to the truck trailer combination (Eui-Seung Hwang, 1991), (Huan Zeng, 2003) with the aid of these references. The continuous-time state-space matrices  $[\mathbf{A}, \mathbf{B}, \mathbf{C}, \mathbf{D}]$  are constructed programmatically along with static deflection matrix  $[\mathbf{x}_0]$ , Stiffness and Damping matrices  $[\mathbf{K}, \mathbf{C}]$  in the MATLAB script (see Appendix B.2), and the Simulink diagram uses a State-Space block that reads these matrices from the base workspace (Appendix C).

#### 3.1 Variables & Parameters

**State vector (20 states).** The state vector comprises the heave and pitch motions of the truck body, denoted by  $y$  and  $\phi_1$  respectively, together with the heave motions of the two unsprung masses, identified by subscripts (front 1, rear 2). In addition, the trailer body heave and pitch motions ( $Y, \phi_2$ ), along with the heave of two unsprung masses on the trailer with subscripts (front 3, rear 4). Finally, the vertical motion and pitch rotation of the drawbar are represented by  $(w, \phi_3)$ . Each generalized coordinate is accompanied by its corresponding velocity, resulting in a total of 20 state variables.

The complete state vector is given by

$$\mathbf{x} = \begin{bmatrix} y \\ \dot{y} \\ y_1 \\ \dot{y}_1 \\ y_2 \\ \dot{y}_2 \\ \phi_1 \\ \dot{\phi}_1 \\ Y \\ \dot{Y} \\ y_3 \\ \dot{y}_3 \\ y_4 \\ \dot{y}_4 \\ \phi_2 \\ \dot{\phi}_2 \\ w \\ \dot{w} \\ \phi_3 \\ \dot{\phi}_3 \end{bmatrix}$$

**Inputs (4 road disturbances).** The input vector consists of four road disturbance signals representing the vertical road excitations acting at the tyre-road contact points over time. These inputs correspond to the front ( $z_1$ ) and rear ( $z_2$ ) wheels of the truck and the front ( $z_3$ ) and rear ( $z_4$ ) wheels of the trailer, respectively. The input vector is

defined as

$$\mathbf{u} = \begin{bmatrix} z_1 \\ z_2 \\ z_3 \\ z_4 \end{bmatrix}.$$

It is also important to note that only  $z_1$  from the input matrix is unique input (Speed bump and Expansion joint profile). The subsequent inputs are corresponding distance delays computed from the vehicle dimensions (distance between axle groups) and travel speed,  $v_x$  meaning  $z_2, z_3, z_4$  are dependent on  $z_1$  and retains the standard state-space formulation. This was implemented using the transport delay function in Simulink.

**Key parameters.** The vehicle model parameters comprise suspension, tyre, mass–inertia, and geometric properties. The suspension and tyre stiffness and damping parameters are defined as

$$\begin{aligned} C_{sf}, D_{sf}, C_{sr}, D_{sr} & \quad (\text{truck susp.}), \\ C_{sft}, D_{sft}, C_{srt}, D_{srt} & \quad (\text{trailer susp.}), \\ C_{wtf}, C_{wtr}, C_{wtf}, C_{wtr} & \quad (\text{tire vertical stiffness}), \\ C_{sd}, D_{sd} & \quad (\text{drawbar coupling}). \end{aligned}$$

The mass, inertia, and geometric parameters include the sprung and unsprung masses of the truck and trailer, the drawbar mass, and the relevant axle and coupling distances:

$$\begin{aligned} m_c, m_{uf}, m_{ur}, m_{ct}, m_{uft}, m_{urt}, m_d, \\ l_f, l_r, l_{ft}, l_{rt}, a_1, a_2, l_{fd}, l_{rd}, \end{aligned}$$

Considering the pitch moment of inertia, the values were derived using a lumped mass model where the body mass is considered concentrated at the center of gravity (CG) and the wheel masses at their respective axles. This gives the approximate value of the moment of inertia as,

$$I_p = m_{frontaxle}l_f^2 + m_{rearaxle}l_r^2$$

This formulation can be approximated as,

$$I_p = \frac{m_{total}(l_f^2 + l_r^2)}{2},$$

The pitch moments of inertia of the truck, trailer, and drawbar are approximated as

$$I_y = \frac{m_c(l_f^2 + l_r^2)}{2}, \quad I_{yt} = \frac{m_{ct}(l_{ft}^2 + l_{rt}^2)}{2}, \quad I_{yd} = \frac{m_d(l_{fd}^2 + l_{rd}^2)}{2}.$$

Road definition uses a constant forward speed  $V_x$  and wavelength  $\lambda$ ,  $\omega = 2\pi V_x/\lambda$ , and fixed axle longitudinal offsets  $s_1, \dots, s_4$  with arrival times  $t_i = s_i/V_x$ .

Nominal numerical values for all parameters are provided in Appendix A and are consistent with those used in the MATLAB implementation. The truck and trailer masses, axle locations, and geometric dimensions were obtained from the Swedish Transport Agency's online vehicle registry (Transportstyrelsen, 2025). Suspension and tyre parameters were assigned based on TruckMaker (IPG Automotive GmbH, 2025) data and supplemented by engineering estimates and representative values given by experts (Industrial PhD Scholars).

## 3.2 Equations of Motion

The vehicle model is formulated as a linear, small-angle vertical–pitch system with heave and pitch degrees of freedom for the truck, trailer, and drawbar, together with four unsprung axle masses. Each suspension group is represented using linear spring–damper elements, and the tire–road interaction is modelled using linear vertical stiffness as per (Jacobson). The drawbar is included as a linear coupling acting in both heave and pitch, see Figure 2.

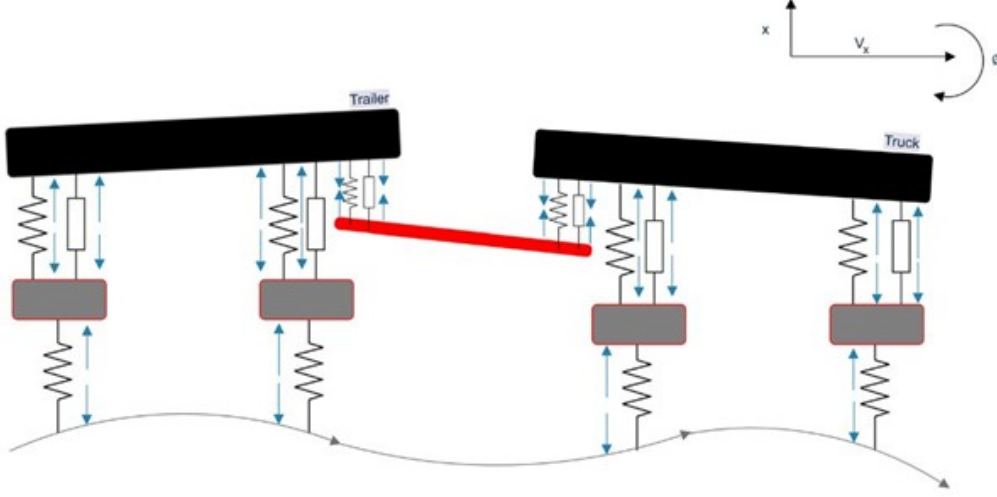


Figure 2: Schematic representation of the truck–trailer–drawbar model showing the masses, suspension elements, drawbar connection, and road input.

A free-body diagram of the truck body, illustrating the forces and moments used in the vertical and pitch equilibrium, is shown in Figure 3.

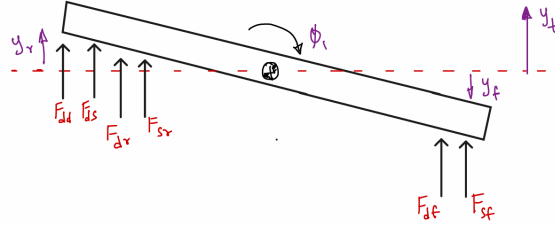


Figure 3: Free-body diagram of the truck body showing the forces and moments considered in the derivation of the equilibrium equations.

To illustrate the modelling approach, the generic suspension and tire force expressions are written as

$$F_{sf} = C_{sf}(y_{uf} - y_c + l_f\phi_c) + D_{sf}(\dot{y}_{uf} - \dot{y}_c + l_f\dot{\phi}_c),$$

$$F_{sr} = C_{sr}(y_{ur} - y_c - l_r\phi_c) + D_{sr}(\dot{y}_{ur} - \dot{y}_c - l_r\dot{\phi}_c).$$

Using these definitions, the full non-linear force balance for each sprung and un-sprung mass, and the drawbar is assembled. The complete system of equations, including the truck heave and pitch, trailer heave and pitch, axle dynamics, and drawbar motion—is

provided in Appendix B.1. These equations form the basis for the state–space representation used in the simulations.

### 3.3 State–space form

With the ordering of the state vector  $\mathbf{x}$  and the inputs  $\mathbf{u}$  defined in Appendix B.2, the system is written in first-order form as

$$\dot{\mathbf{x}} = \mathbf{A}\mathbf{x} + \mathbf{B}\mathbf{u}, \quad \mathbf{y} = \mathbf{C}\mathbf{x} + \mathbf{D}\mathbf{u}.$$

The matrices  $\mathbf{A} \in R^{20 \times 20}$  and  $\mathbf{B} \in R^{20 \times 4}$  contain all suspension, tire, and drawbar coupling terms and sets  $\mathbf{C} = \mathbf{I}_{20}$ ,  $\mathbf{D} = \mathbf{0}_{20 \times 4}$ . For clarity, these matrices are not expanded here; the exact symbolic expressions and numerical assembly are provided in the modelling script (Appendix B.2).

### 3.4 Simulink Implementation

The Simulink model uses a State-Space block whose parameters are the workspace variables  $\mathbf{A}$ ,  $\mathbf{B}$ ,  $\mathbf{C}$ ,  $\mathbf{D}$ . Before each simulation, a MATLAB pre-simulation callback computes these matrices from the current parameter set and assigns them to the base workspace.

Road inputs  $z_f, z_r, z_{ft}, z_{rt}$  are provided as external excitations. Signal logging is enabled to collect the full state vector and derived quantities such as tire contact forces. The Simulink implementation is presented in Appendix C.

## 3.5 Experiments

### 3.5.1 TruckMaker Simulations

To complement the analytical and Simulink-based model, similar driving scenarios were simulated in *TruckMaker* (IPG Automotive GmbH, 2025). The purpose was to obtain representative dynamic responses and parameter estimates under realistic vehicle and road conditions.

Based on manufacturer data and nominal configuration parameters, a virtual prototype of the reference vehicle was constructed. The suspension, steering, and tire subsystems were parameterized according to available documentation and calibration data, enabling the model to capture the dominant nonlinear characteristics of the sprung mass motion, unsprung mass dynamics, and tire–road interaction. This high-fidelity representation serves as a reliable benchmark for identifying the reduced-order equivalent parameters.

A set of controlled driving scenarios was executed on a predefined test route. The scenarios included constant-velocity cruising, small-amplitude steering inputs, and transient disturbances introduced through road excitations. These inputs were selected to sufficiently excite the vertical and longitudinal dynamics while avoiding excessive nonlinearities or numerical artefacts.

All simulations were performed using a high-resolution fixed-step solver in *TruckMaker*. For each scenario, key variables—including heave, pitch, and roll motions of the chassis, wheel-hub kinematics, and suspension forces—were recorded. These time-domain responses form the basis for identifying the equivalent linear stiffness, damping, and inertia parameters.

From these simulations, equivalent stiffness and damping values were extracted for use in the simplified state-space model, see Appendix A.

### 3.5.2 Simulink Simulations

Simulink was set up for the two different road cases (see Appendix C for the Simulink block diagram). To compare the result from Truckmaker.

### 3.5.3 Road profile

The road was modeled as a smooth profile without any disturbances apart from the two scenarios (Bump and Expansion joint). A detailed explanation on how the disturbances were modeled is available in Appendix D.

### 3.5.4 Load and Velocity Sweep

To investigate how operating conditions influence the dynamic response of the truck–trailer combination, a systematic sweep over vehicle load and forward velocity was implemented over two road surfaces. In contrast to a traditional parameter-uncertainty study, no suspension or structural parameters were altered. Instead, only the total load mass and vehicle speed were varied.

Three load conditions were evaluated:

- No load (empty vehicle),
- Half load,
- Full load.

Each load case was simulated at five forward velocities:

$$V_x = 5, 10, 15, 20, 25 \text{ m/s.}$$

The simulations were done in these speed range because it is the typical speeds that the truck travels (max 90 Km/hr). For every load–velocity combination, the mass parameters were updated and the state–space matrices **A**, **B**, **C**, **D** were recomputed using the pre-simulation MATLAB function. The model was then simulated using Simulink Fast Restart, with all relevant states and outputs recorded for later analysis. The complete configuration of the sweep is documented in Appendix D.

## 4 Results

### 4.1 Overview

The Timber truck–trailer simulation study was conducted for three different loading configurations, six vehicle velocities, and two distinct road excitation profiles representing a bump and a step. The results obtained across these scenarios show consistent and realistic system behaviour, demonstrating that the modelling framework successfully captures the essential dynamics of the heavy vehicle combination.

The vertical forces generated at the axle–road interfaces under all conditions provide valuable insight into the coupled behaviour of the vehicle and the bridge. By analysing these responses, the natural frequencies of both the truck–trailer system and the bridge structure can be compared, allowing the identification of potential resonance risks and critical operating conditions. Furthermore, the simulated results serve as a basis for comparison with experimental test data. This comparison strengthens confidence in the model’s predictive capability and enhances the understanding of how increased loading—associated with the upgraded 74-ton trucks—affects bridge performance.

Overall, the results give a clear picture of how the upgraded bridge responds to higher vertical forces induced by heavy vehicles. This understanding is crucial for determining safe vehicle operating speeds during bridge crossing, minimising vibration levels, and ensuring long-term structural health. The outcomes of the study contribute to establishing guidelines and operational limits that support both traffic safety and extended bridge service life.

### 4.2 Simulations

The inputs are fully defined in the simulation such as

- Fixed vehicle speed
- Fixed axle loads
- Fixed road profile (bump profile and Road and Bridge Expansion Joint)
- Fixed geometry
- Fixed suspension parameters

This predefined condition used to study vehicle-bridge interaction.

#### 4.2.1 Simulation Setup

The simulation is performed using below mentioned setup.

##### 1. Vehicle model Setup

- Truck-trailer configuration(no of axle, spacing, suspension parameters).
- Mass configuration (light, medium, full load).
- Tire parameters(Stiffness and Damping coefficient)
- Drawbar connection
- Dof considered (heave, pitch, bounce)

##### 2. Road excitation profiles

- Bump profiles (geometry)
- step profile (geometry)

### **3. Simulation parameter**

- Vehicle speed (5 predefined velocities)
- Simulation duration and time step.
- Assumption of deterministic inputs

These simulation serve as baseline for accessing the dynamic amplification factor and validating the vehicle response before comparing the results with experimental measures.

#### **4.2.2 Time-Domain Responses**

The Time-domain response describes the actual simulation results over time.

##### **1.Vertical displacement of Truck-Trailer and Drawbar bodies**

- Heave,pitch motion.
- Response differences between load cases.

##### **2.Wheel vertical displacement**

- How each axel is response to bump/step profiles
- Identification of peak response

##### **3.Vertical dynamic forces at each axle(Vehicle bridge interaction)**

- Time-varying wheel road contact forces.
- peak forces and oscillation.
- Difference for speed, load and profiles

##### **4. Identification of critical events**

- maximum input force at entry at step and later bump profiles.
- Rebound oscillation.
- when resonance appears.

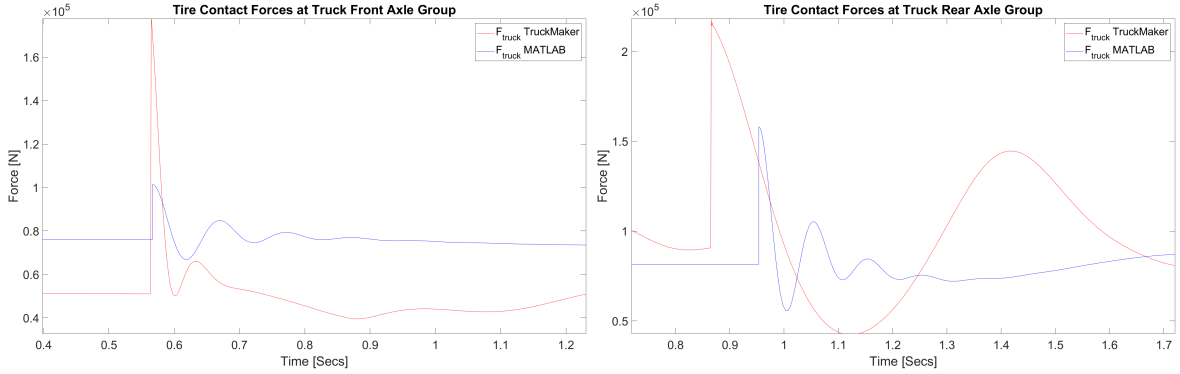
The oscillatory behaviour observed in the time histories reflect the natural frequency of both the bridge and vehicle, enabling identification of potential resonance conditions and these responses form the basic for calculatg the DAF and compare the forces with the experimental test data.

### **4.3 Model Validation**

To validate the developed model before proceeding with further testing, a comparison was carried out between the model and the commercial simulation software TruckMaker. The objective of this comparison was to ensure that the implemented model exhibits similar dynamic behaviour under equivalent conditions.

Since the parameters in TruckMaker cannot be modified directly, the parameters in the developed model were adjusted to match those used in TruckMaker as closely as possible during the validation.

When plotting the tire contact forces for the truck’s front and rear axle group from the project model and TruckMaker, the peak forces were not the same as expected, the settling times were different due to the complexity of the model in TruckMaker, but the number of peaks and the response for both the cases were similar.



(a) Front axle group MATLAB Vs TruckMaker,  $V = 15$  m/s (b) Rear axle group MATLAB Vs TruckMaker,  $V = 15$  m/s

Figure 4: Comparison of Tire contact forces for the FullLoad configuration over the Expansion joint for Truck

For the trailer, the same considerations apply. The response from both the models were similar. The main purpose of the project is to assess the influence of the contact forces for different load cases and velocities over the bridge and since it is a comparative study, the model developed will provide the same intuition when compared with a commercial software. For instance, adding complexity to the model like non-linear spring and damper, tire models, road profiles will give results identical to the validation software, but the goal is flexibility in the model which TruckMaker lacks.



(a) Front axle group MATLAB Vs TruckMaker,  $V = 15$  m/s (b) Rear axle group MATLAB Vs TruckMaker,  $V = 15$  m/s

Figure 5: Comparison of Tire contact forces for the FullLoad configuration over the Expansion joint for Trailer

#### 4.4 Load and Velocity Sweep Results

To quantify how the truck–trailer system responds to different dynamic conditions, a sweep of 30 operating points was simulated: three load cases (*FullLoad*, *HalfLoad*, *NoLoad*) and five velocities (5–25 m/s). For each combination, the vehicle was subjected to two road disturbances:

- a **speed bump** input, representing a short-wavelength and high-amplitude excitation,
- a **bridge expansion joint / road step** input, representing a sharp discontinuity in the road surface.

The complete collection of response plots and road inputs is provided in Appendix D. In the following, representative cases are shown to highlight the effects of loading and speed on the resulting tire forces.

### Overview of the results:

From the plots of Amplification factor vs velocity, for the no load case, the amplifications is high but the peak force is low. The amplification is velocity dependent for the case of the speed bump while the it is nearly constant in the case of the expansion joint disturbance.

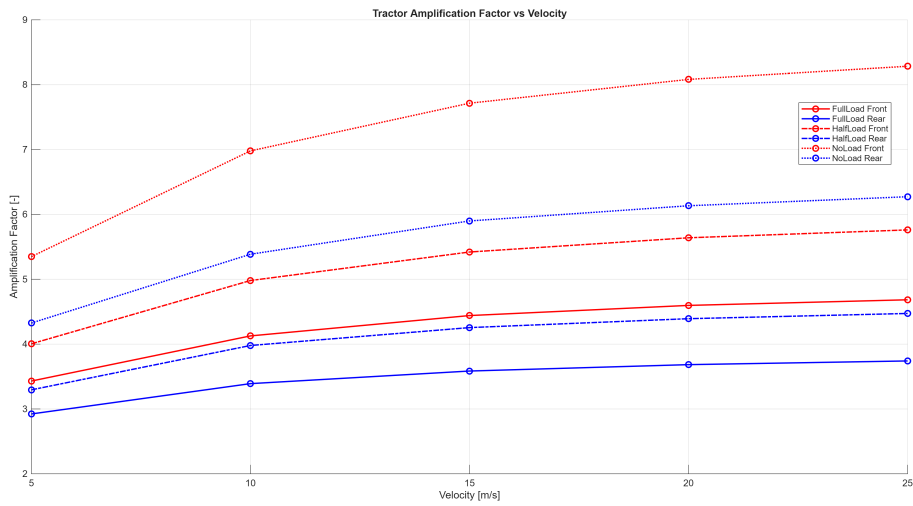


Figure 6: Speed Bump truck AF

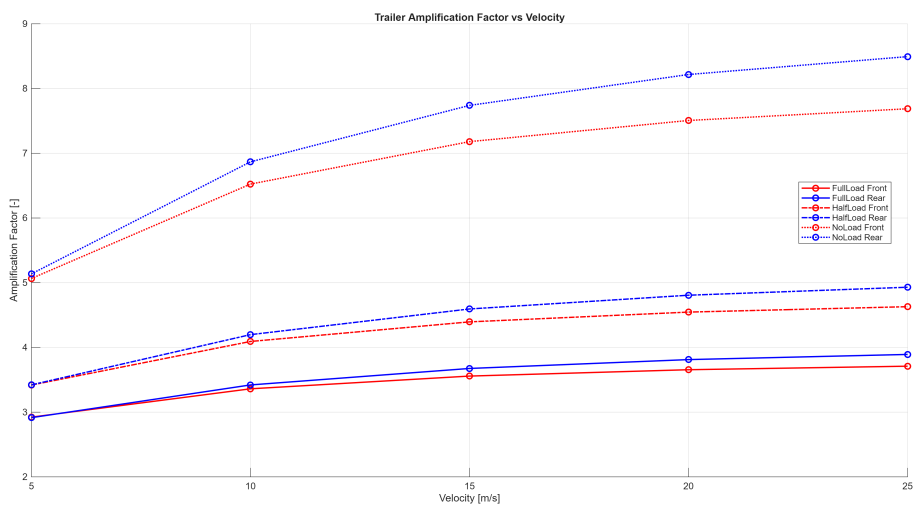


Figure 7: Speed Bump Trailer AF

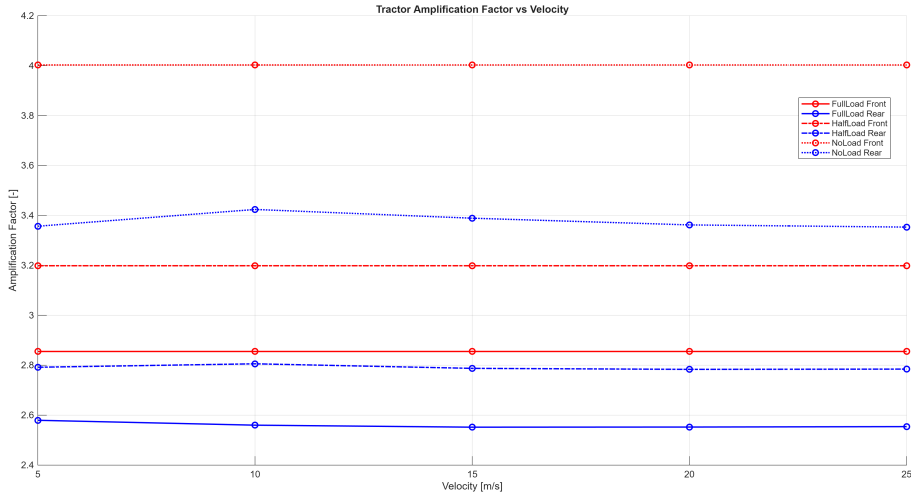


Figure 8: Expansion Joint truck AF

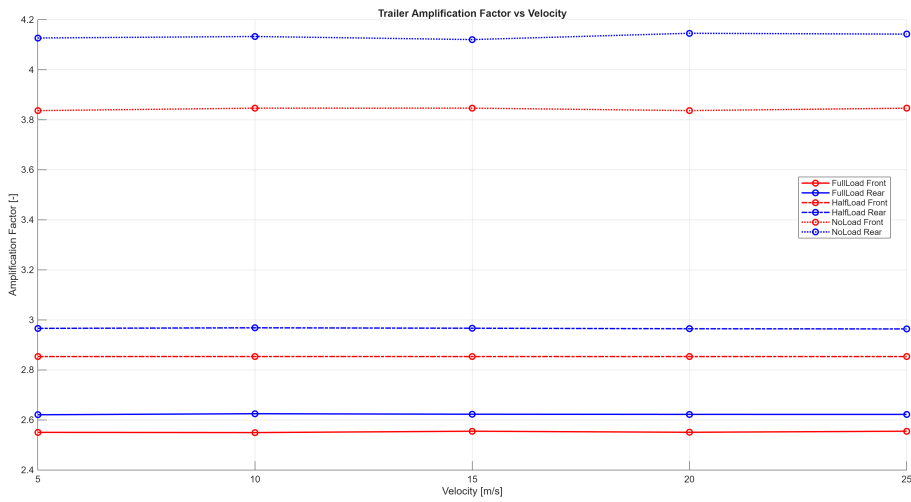


Figure 9: Expansion Joint Trailer AF

Low speed takes the longest to stabilise see Appendix .

#### 4.4.1 Effect of Load

The vehicle load influences the natural frequencies, damping ratios, and force transmission characteristics. To illustrate this clearly, the figures below compare the *FullLoad* and *NoLoad* conditions at a representative operating speed of 20 m/s (72 km/h).

#### CASE – 1: Speed Bump

Figures 10–11 compare the FullLoad and NoLoad responses at 20 m/s. As seen in the figures, the lighter vehicle exhibits:

- significantly higher peak dynamic tire forces,
- faster and more oscillatory response,
- a shorter decay time due to lower overall mass.

In contrast, the FullLoad configuration produces:

- lower peak force amplification,

- smoother overall force curves,
- slower, more heavily damped oscillations driven by larger inertia.

This shows that heavy loading tends to attenuate the high-frequency dynamics but increases the static force baseline carried by the axles.

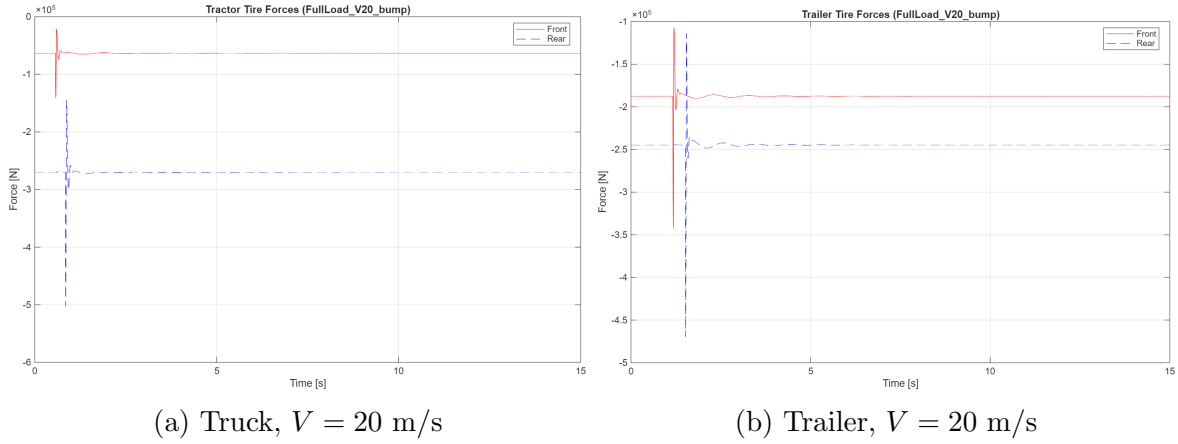


Figure 10: Tire contact forces for the FullLoad configuration over the bump profile at  $V = 20$  m/s.

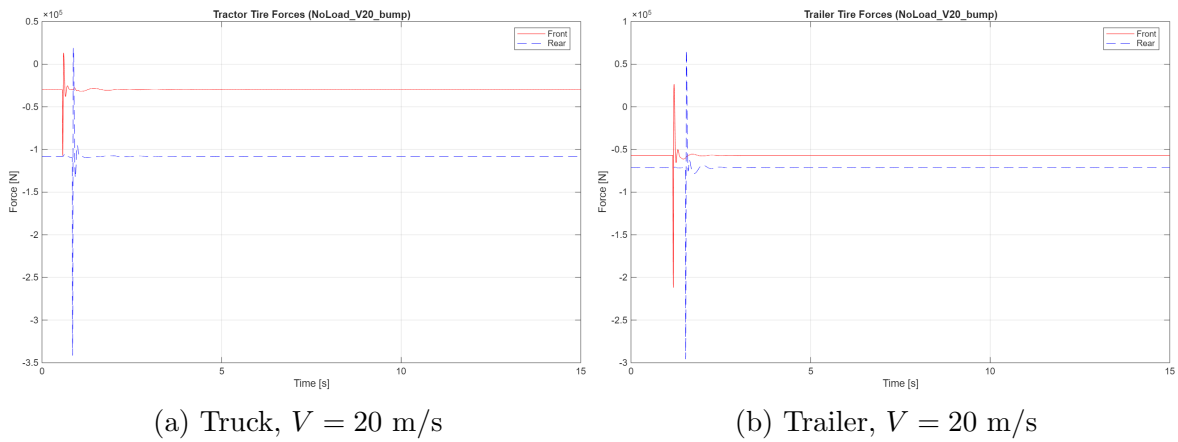


Figure 11: Tire contact forces for the NoLoad configuration over the bump profile at  $V = 20$  m/s.

## CASE – 2: Road & Bridge Expansion Joint

Figures 12–13 show the step-input response at 20 m/s. The step introduces a very sharp impulse followed by oscillations.

In the NoLoad case, the force peaks are distinctly higher and the oscillations more pronounced. The FullLoad system shows a muted peak and a smoother recovery.

Compared to the bump case, the step excitation:

- produces a shorter-duration, sharper impulse,
- excites mainly the high-frequency unsprung modes,
- results in less sustained oscillatory behaviour in the trailer axles.

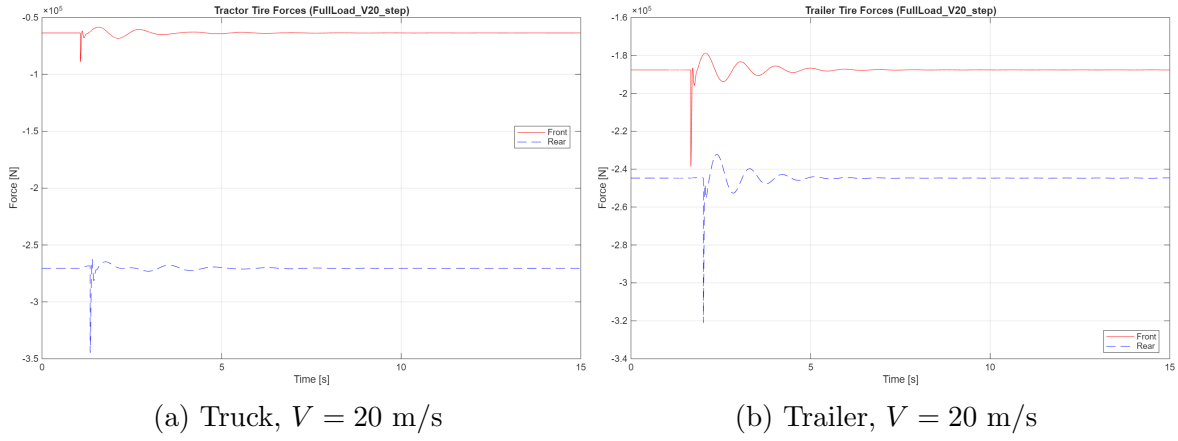


Figure 12: Tire contact forces for the FullLoad configuration over the step profile at  $V = 20$  m/s.

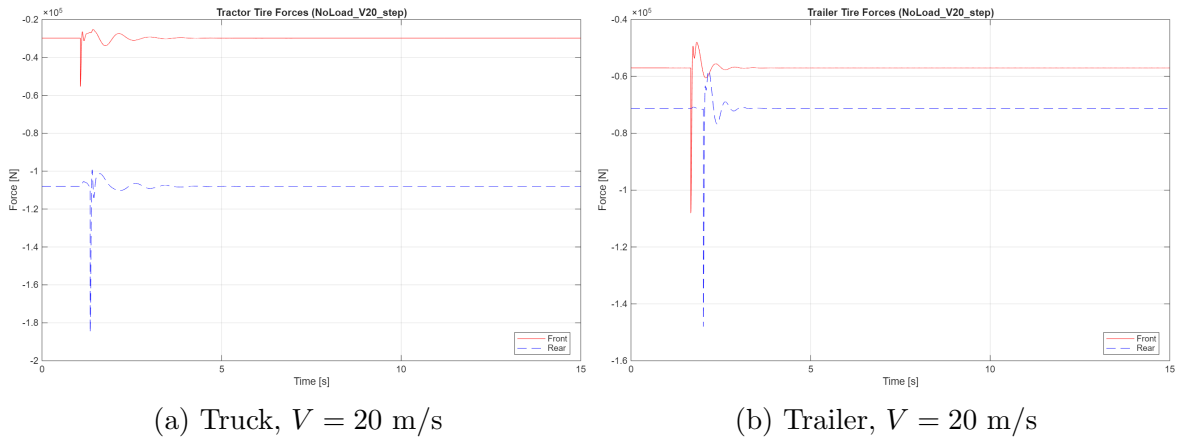


Figure 13: Tire contact forces for the NoLoad configuration over the step profile at  $V = 20$  m/s.

#### 4.4.2 Effect of Velocity

Vehicle speed directly affects the frequency content and severity of road-induced load inputs. At low speeds, the excitation is relatively slow and the chassis has time to respond quasi-statically. As the speed increases, the excitation effectively shifts toward higher frequencies and shorter effective wavelengths, amplifying dynamic forces and reducing the time available for suspension deflection.

To illustrate this, the following figures show the response for the FullLoad configuration at the lowest and highest simulated speeds: 5 m/s and 25 m/s.

#### CASE – 1: Speed Bump

Figures 14–15 illustrate how vehicle speed shapes the dynamic forces.

- At **5 m/s**, the bump is encountered slowly, giving a mostly smooth and quasi-static response with low peak forces.
- At **25 m/s**, the bump input becomes a high-frequency excitation, producing:
  - a sharp transient peak immediately after contact,
  - a noticeable increase in peak dynamic force,

- shorter, higher-frequency oscillations,
- larger amplification for the trailer rear axle.

Thus, increasing speed significantly increases dynamic amplification for both truck and trailer axles.

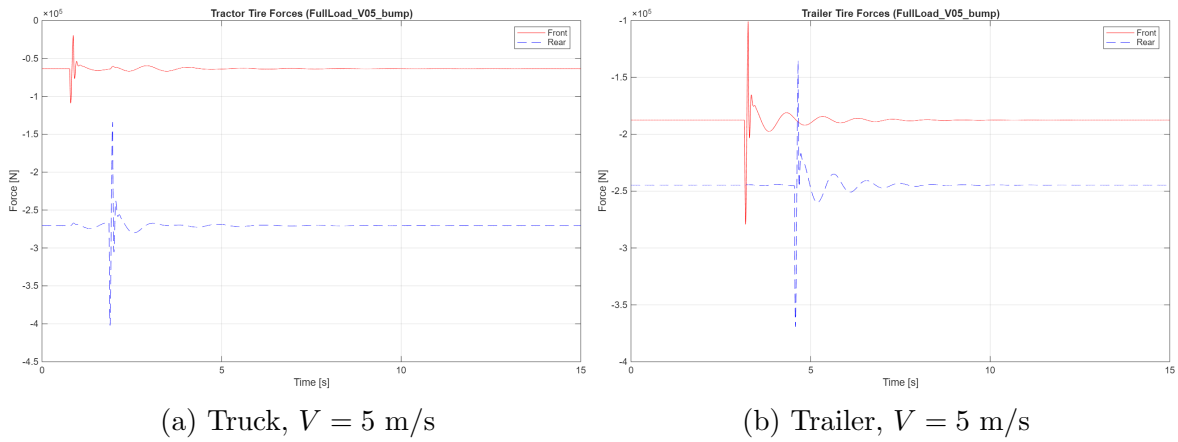


Figure 14: Tire contact forces for FullLoad over the bump profile at  $V = 5$  m/s.

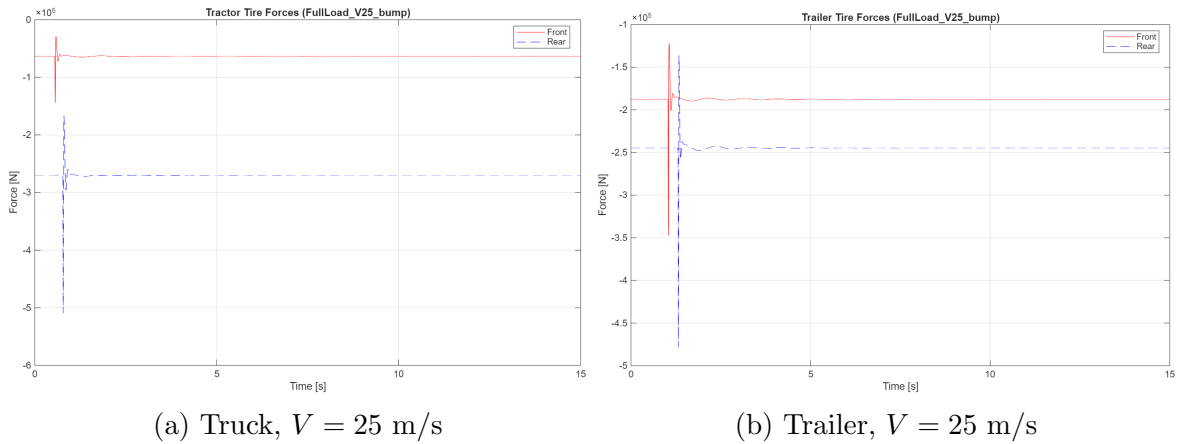


Figure 15: Tire contact forces for FullLoad over the bump profile at  $V = 25$  m/s.

## CASE – 2: Road & Bridge Expansion Joint

Figures 16–17 show the effect of velocity in the step-input case.

- At **5 m/s**, the step input generates a relatively small impulse with mild oscillations.
- At **25 m/s**, the system encounters the step almost instantaneously, resulting in:
  - a sharp, high-magnitude tire-force spike,
  - reduced duration of oscillations,
  - a clear difference between tractor and trailer response due to their different suspension stiffnesses and inertias.

Compared to the bump case, the step response at high speed is dominated by a single large impulse rather than multiple oscillations.

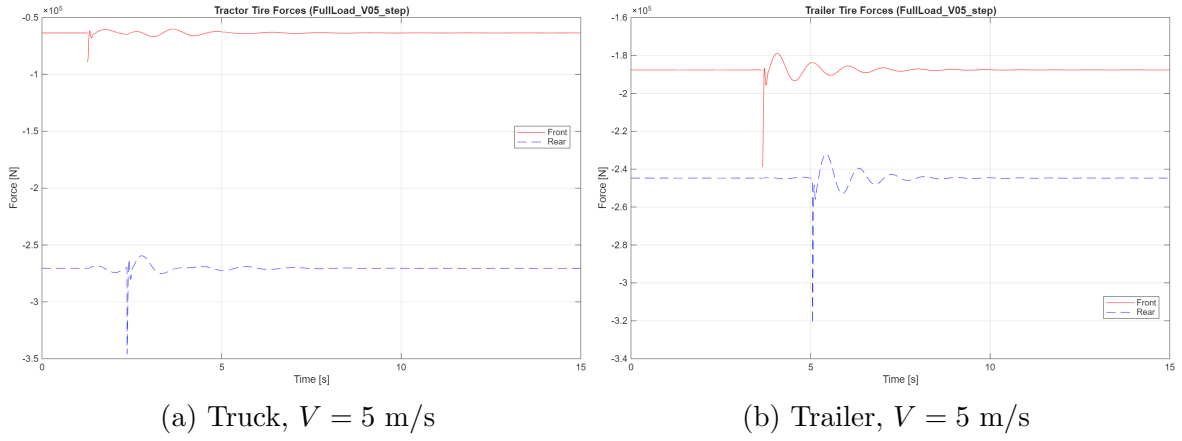


Figure 16: Tire contact forces for FullLoad over the step profile at  $V = 5$  m/s.

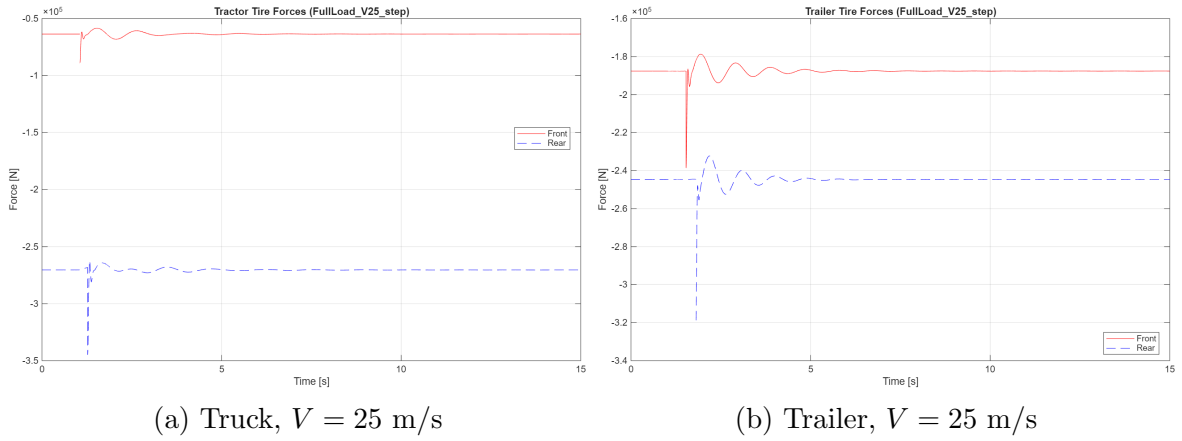


Figure 17: Tire contact forces for FullLoad over the step profile at  $V = 25$  m/s.

## 4.5 Dynamic Amplification Factor (DAF)

The fundamental understanding on DAF was obtained from (Arturo González, 2018) and (CHRISTOFFER SVEDHOLM, 2021) and its effect on the design and lifetime of the bridge was important to consider.

$$DAF = F/S$$

for 15, 20 ,25 m/s

According to Trafikverket (Trafikverket, 2025), the dynamic amplification is given by Equation (8–1) in Section 8.3.2.2.2.

$$D = \frac{180 + 8(v - 10)}{20 + L} [\%] \quad (1)$$

The dynamic length for  $n = 3$  may be determined using the expression given in Bilaga 2 in Trafikverket (2025).

$$l_m = \frac{1}{n} \cdot (l_1 + l_2 + \dots + l_n) [m] \quad (2)$$

$$L = 1.3 \cdot l_m [m] \quad (3)$$

The length of the bridge span is 10m and the height of the two supports is 8m, see Figure 18.

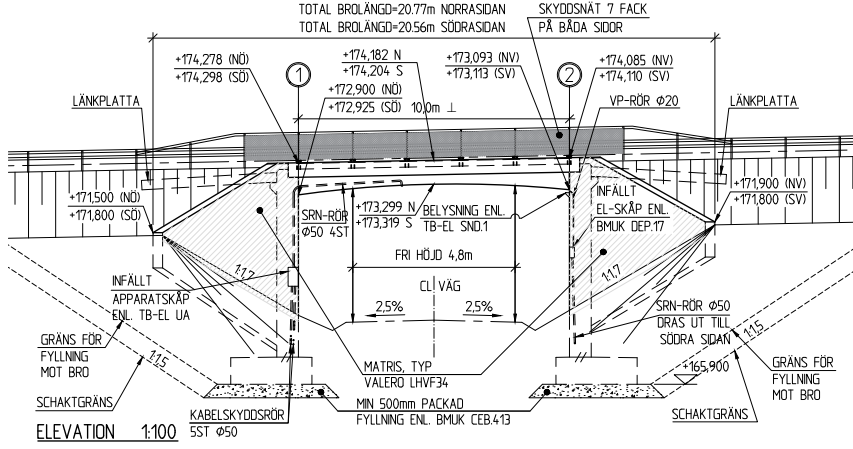


Figure 18: Bridge dimensions

$$l_m = \frac{1}{3} \cdot (8 + 10 + 8) = 8.667[m] \quad (4)$$

$$L = 1.3 \cdot 8.667 = 11,267[m] \quad (5)$$

The dynamic amplification is then for  $v = 80\text{km/h}$ :

$$D = \frac{180 + 8(80 - 10)}{20 + 11,267} [\%] = 31,267 \quad (6)$$

## 4.6 Summary of Key Findings

The developed model is well suited for studying the influence of vehicle speed, loading condition, axle configuration, and road profile characteristics on dynamic tire forces and force amplification. The time-domain force outputs can be readily transformed into the spatial domain and applied as moving loads in bridge models, making the approach particularly applicable for preliminary bridge dynamic analysis and vehicle-bridge interaction studies. Due to the simplified linear suspension and tire representations and the point-contact assumption, the model is not intended for precise prediction of absolute peak loads under highly nonlinear or extreme conditions. Instead, it serves as an efficient reduced-order tool for trend analysis, sensitivity studies, and comparative evaluation, providing valuable insight into the dominant mechanisms governing dynamic axle loads on bridges.

## 5 Discussion

This project focused on the development, analysis, and evaluation of a mathematical model describing the dynamic behaviour of a vehicle system. The primary emphasis was on deriving a physically meaningful yet computationally efficient model that captures the essential dynamics of the vehicle under various operating conditions.

The work began with a detailed study of vehicle dynamics theory, followed by the formulation of the governing equations of motion using fundamental principles such as Newton's laws. To simplify the modelling process while retaining accuracy, certain assumptions were made, including lumping axle groups and neglecting higher-order effects that have minimal influence on the system response within the considered operating range.

Relevant vehicle parameters such as mass distribution, suspension stiffness, damping coefficients, and geometric properties were identified based on available data from the Swedish Transport Agency's online registry (Transportstyrelsen, 2025) and TruckMaker (IPG Automotive GmbH, 2025). These parameters were then implemented into the simulation environment to construct a representative vehicle model.

Deterministic simulations were carried out for different loading conditions, vehicle speeds, and road profiles. Time-domain responses were analyzed to evaluate key dynamic behaviours such as vertical displacement and pitch motion. The simulation results were systematically compared with TruckMaker (IPG Automotive GmbH, 2025) data to assess the validity and robustness of the developed model.

### 5.1 Interpretation of Model Behaviour

The developed vehicle model exhibits physically consistent behaviour across all scenarios. The time-domain responses show that the vehicle system reacts predictably to changes in road excitation, load conditions, and vehicle speed. Vertical and pitch motions remain within reasonable limits, indicating stable dynamic behaviour and the absence of numerical instabilities.

The coupling between the motion of the sprung mass and the dynamics of the axle is clearly reflected in the simulation results. Road-induced disturbances are transmitted through the suspension system, resulting in characteristic oscillatory responses that are governed by the suspension stiffness and damping properties. Increased road excitation leads to higher vertical accelerations and displacement amplitudes, while damping plays a critical role in limiting oscillation duration and ensuring acceptable settling times.

Overall, the behaviour of the model aligns well with theoretical expectations of vehicle dynamics, confirming that the underlying equations of motion, parameter selection, and modelling assumptions are appropriate for the intended scope of the study. The results provide confidence that the model can be reliably used for system-level analysis and further model development.

### 5.2 Comparison with TruckMaker

Given that the project timeline did not permit physical bridge testing with a real vehicle, the validation process presented significant challenges. To address this, the performance of the developed model was evaluated using a commercial simulation software, IPG TruckMaker, as a ground truth reference.

It is also important to note that the exact truck and trailer configuration (dimensions, design) wasn't available in the simulation software, so the developed model's parameters were altered to match the available product example. In addition, an important consideration the model avoids is tire contact patch modeling, which will have a significant influence in the contact forces. The model in MATLAB assumes point contact whereas TruckMaker has its own non-linear tire model in built. Due to these discrepancies, it will be unfair to expect exact force values and peak occurrences. The main objective to confirm whether the developed model has acceptable dynamics response in comparison with the commercial software.

### 5.3 Influence of Load and Velocity

The load carried by the truck trailer combination apart from its kerb weight and its travel speed will have a significant effect on the peak force values over different road profiles. To analyse this effect, three load cases (Full load, Half load and No load) and a range of longitudinal velocities (5 m/s - 25 m/s) were considered. The tire contact forces for all the cases were simulated.

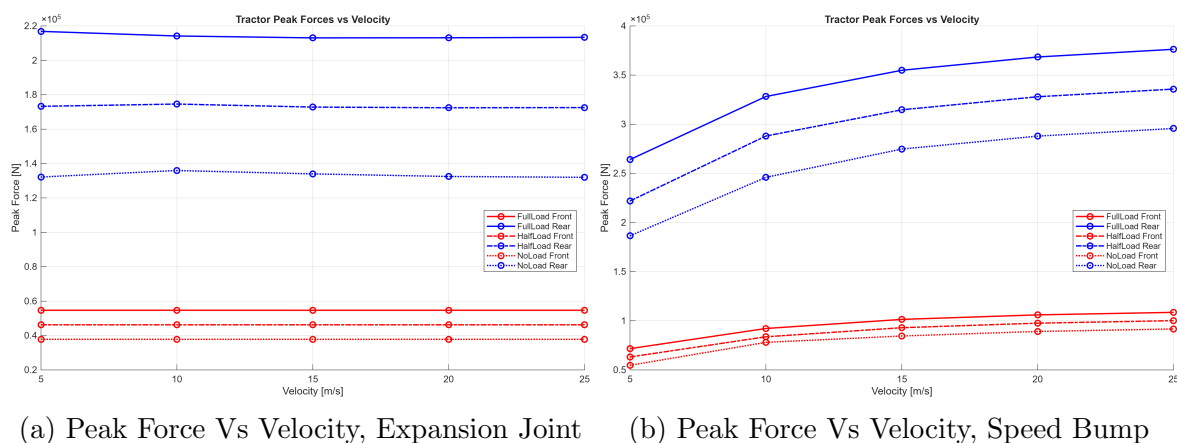


Figure 19: Tire contact forces of the Truck's front and rear axle groups for the two different road disturbances

The above plots show the effect of different load cases and velocities on the tire contact force. It was observed that for the Expansion joint, the peak force was almost independent of the velocity (near same values). This maybe due to the very short step input (30 mm) and also since the road disturbance is not a function of the longitudinal velocity in the Simulink model. Whereas, for the speed bump the peak force was directly dependent on the longitudinal velocity. Due to the difference in the total mass of the combination, the peak force values were high for Full load case and low for No load case.

### 5.4 Limitations of the Model

The MATLAB/Simulink model developed in this project is based on a linear spring-damper system which represents the vertical and pitching dynamics of the half-truck, trailer, and drawbar system. Suspension components and tires are assumed to behave linearly with constant stiffness and damping, whereas real systems exhibit load-dependent and nonlinear behavior. The tire-road interaction is modeled as a point contact with linear vertical stiffness, neglecting the finite tire contact patch, wheel enveloping effects, and frequency-dependent tire characteristics. As a result, high-frequency force content and peak tire

forces may be overestimated, particularly for short-wavelength or abrupt road inputs such as speed bumps or step profiles.

Furthermore, the model considers only vertical and pitch motions and assumes rigid bodies for the truck, trailer, and drawbar, thereby neglecting structural flexibility and higher-frequency vibration modes. Lateral and longitudinal dynamics, braking and acceleration effects, and wheel lift-off are not included, and vehicle speed is assumed constant throughout the simulation. Static loads are introduced through simplified preloading or post-processing, and interaction between the vehicle and a flexible supporting structure, such as a bridge, is not modeled. Consequently, while the model is computationally efficient and well suited for parametric studies and trend analysis, it cannot fully capture detailed tire behavior, nonlinear suspension effects, or vehicle–bridge coupling present in real-world scenarios.

## 5.5 Reliability and Applicability of the Results

The results obtained in this study are considered reliable within the assumptions and scope of the developed MATLAB/Simulink model. The vehicle dynamics model is based on well-established formulations for vertical and pitching motion and uses physically representative parameters for the timber truck, trailer, and drawbar system. Static equilibrium conditions were incorporated through preloaded suspension elements, ensuring that the dynamic response is evaluated about a realistic operating point. Parametric studies across different vehicle speeds and loading conditions produced consistent and physically meaningful trends, indicating good internal robustness of the model. Qualitative comparison with high-fidelity Truck-Maker simulations showed agreement in the dynamic response, and relative force amplification, supporting the credibility of the obtained results despite differences in absolute peak values.

Furthermore, the numerical stability of the model across all simulated scenarios strengthens confidence in the reliability of the results. No unphysical oscillations or divergence were observed, even under high load and velocity conditions, indicating that the governing equations and parameter values are well-conditioned. The sensitivity of the system response to changes in load and speed follows established vehicle dynamics theory, further validating the correctness of the implemented model structure.

While the model does not aim to replicate all nonlinear effects captured by high-fidelity Truck-Maker software, it successfully reproduces the dominant vertical and pitch dynamics that govern ride response and load transfer in heavy vehicle combinations. This makes the model particularly suitable for comparative studies, early-stage design evaluations, where insight into system behaviour is more important than exact numerical accuracy.

In summary, within its defined assumptions and modelling scope, the developed MATLAB/Simulink model provides reliable and meaningful results that are suitable for system-level analysis and serve as a solid basis for further refinement and higher-fidelity modelling efforts.

## 6 Conclusions

From the results obtained, it can be concluded that the developed vehicle dynamics model successfully captures the essential contact force of tyre with the bridge under a wide range of operating conditions. The model demonstrated stable and physically consistent responses for different vehicle speeds, road excitations, and load cases.

The simplification approach adopted—particularly the lumping of axle groups—proved to be effective in reducing model complexity while maintaining sufficient accuracy for system-level analysis. This confirms that such modelling assumptions are justified during the early design and analysis stages.

The time-domain simulation results showed reasonable agreement with TruckMaker (IPG Automotive GmbH, 2025) data, indicating that the chosen parameters and modelling methodology are appropriate. Variations observed between different loading and speed conditions were consistent.

Overall, the project met its primary objectives by deriving contact forces of tyres on different load, road and vehicle speed which will be further used for the study of the vehicle-bridge interaction.

## 7 Future work

The tyre contact forces calculated from the truck–trailer dynamic model will serve as input loads for the bridge dynamic analysis. Since the vehicle model adopts a half-vehicle assumption, the simulated forces represent the vehicle dynamics in the longitudinal plane of symmetry only. Consequently, in the bridge model, the wheel loads will be applied as two lateral load sets and spatially distributed according to the actual vehicle wheelbase and track width, thereby providing an equivalent representation of the full-vehicle loading effects on the bridge.

The loads will traverse the bridge as moving loads, with their positions updated according to the vehicle speed. This enables systematic investigation of bridge response patterns under different speed conditions.

The DAF will be used as a key metric to quantify dynamic effects. It is defined as the ratio between the maximum dynamic response and the corresponding static response, and will be evaluated based on strain and displacement results obtained from the Abaqus simulations.

Future work will include full-scale experimental testing, with sensors installed on both the selected bridge and the timber truck–trailer combination to capture real-world dynamic response data. Tests will be conducted to investigate the effects of road irregularities such as expansion joints and speed bumps under varying vehicle speeds and load conditions.

Measured data from these tests will be used to tune and refine the vehicle model parameters. In this phase, experimental measurements will replace TruckMaker simulations as the primary reference for validation of the MATLAB-based model.

The model can be extended to simulate traffic scenarios involving multiple vehicles, provided that vehicle spacing and constant velocities are known. The constant-velocity assumption simplifies such analyses and makes it easier to obtain the force values as a function of position on the bridge.

Further improvements include the introduction of more realistic road profiles, representing different road quality classes. This would allow the evaluation of vehicle forces under more representative operating conditions, beyond idealized smooth roads with isolated disturbances such as expansion joints or speed bumps.

## References

- Env 1991-3: Traffic loads on bridges – background and notes for guidance, 1994. For spans shorter than 15 m, local irregularities are represented by a 30 mm thick plank, e.g., a surface defect or missing joint element.
- Omar Mohammed Arturo González. Dynamic amplification factor of continuous versus simply supported bridges due to the action of a moving vehicle. <http://www.mdpi.com/journal/infrastructures>, 2018. doi: <http://dx.doi.org/10.3390/infrastructures3020012>.
- MARIO PLOS MATS KARLSSON CHRISTOFFER SVEDHOLM, VIKTOR ERIKSSON. Pre-study of dynamic amplification factor for existing road bridges. Report, Chalmers University of Technology, Chalmers University of Technology, Sweden, 2021.
- Andrzej S.Nowak Eui-Seung Hwang. Simulation of dynamic load for bridges. *Journal of Structural Engineering*, 117(5):25811, 1991.
- Shenbo Yu Gang Wang, Changzheng Chen. Optimization and static output-feedback control for half-car active suspensions with constrained information. *Journal of Sound and Vibration*, 2016.
- Charles W. Bert Huan Zeng. Dynamic amplification of bridge/vehicle interaction: A parametric study for a skewed bridge. *International Journal of Structural Stability and Dynamics*, 3(1):71–90, 2003.
- IPG Automotive GmbH. Truckmaker. <https://www.ipg-automotive.com/en/products-solutions/software/truckmaker/>, 2025. Accessed: November 2025.
- Bengt Jacobson. Vehicle motion engineering. URL [https://research.chalmers.se/publication/543173/file/543173\\_Fulltext.pdf](https://research.chalmers.se/publication/543173/file/543173_Fulltext.pdf). Last updated: 2024-10-07.
- Sultan Mahamdnur. Dynamic analysis and control simulation of half car model active suspension system. Thesis report, JIMMA INSTITUTE OF TECHNOLOGY, JIMMA INSTITUTE OF TECHNOLOGY, ETHIOPIA, 2019.
- Trafikverket. Bro och broliknande konstruktion: Bärighetsberäkning. Technical Report TRVINFRA-00331, Trafikverket, Borlänge, Sweden, July 2025. Publicerad 2025-07-01. Infrastrukturregelverk.
- Transportstyrelsen. Fordon och fordonsägare – fordonsavgifter via registreringsnummer, 2025. URL <https://fordon-fu-regnr.transportstyrelsen.se/>. Accessed: October 10 2025.
- Henrik von Hofsten, Thomas Parklund, Gert Adolfsson, and Dan Lindström. Bk4-utvecklingen på det svenska vägnätet: Positiv utveckling mot ett allt starkare vägnät men mycket arbete kvarstår. Arbetsrapport 1222-2024, Skogforsk, Uppsala Science Park, Sweden, 2024. Foto: Lars Eliasson, Skogforsk.
- Katarina Wik. Uppdatering av regeringsuppdrag – implementering av bärighetsklass 4. PM, Ärendenummer TRV 2020/44448, 2025. Dokumentdatum: 2025-03-05.

# Appendices

## A Parameter list

The truck and trailer parameter values were primarily obtained from simulations performed in TruckMaker (IPG Automotive GmbH, 2025) and from the Swedish Transport Agency’s online vehicle registry (Transportstyrelsen, 2025), using specific registration numbers corresponding to a representative timber truck and trailer combination. These registrations were used only to ensure realistic mass, geometry, and axle configurations for the simulation model. The exact license plates are recorded internally within the project documentation and are not disclosed here, as future field tests may involve different vehicles depending on bridge access restrictions and weight limitations.

Table 2: Full list of model parameters

Parameter	Symbol	Value	Unit
<b>— Truck suspension —</b>			
Front stiffness	$C_{sf}$	200,000	N/m
Front damping	$D_{sf}$	12,000	Ns/m
Rear stiffness	$C_{sr}$	600,000	N/m
Rear damping	$D_{sr}$	36,000	Ns/m
<b>— Trailer suspension —</b>			
Front stiffness	$C_{sft}$	500,000	N/m
Front damping	$D_{sft}$	26,000	Ns/m
Rear stiffness	$C_{srt}$	750,000	N/m
Rear damping	$D_{srt}$	39,000	Ns/m
<b>— Drawbar coupling —</b>			
Vertical stiffness	$C_{sd}$	$6.0 \times 10^6$	N/m
Vertical damping	$D_{sd}$	$5.0 \times 10^4$	Ns/m
<b>— Tire stiffness/damping —</b>			
Truck front tire stiffness	$C_{wf}$	$8.5 \times 10^5$	N/m
Truck rear tire stiffness	$C_{wr}$	$2.55 \times 10^6$	N/m
Trailer front tire stiffness	$C_{wtf}$	$1.70 \times 10^6$	N/m
Trailer rear tire stiffness	$C_{wtr}$	$2.55 \times 10^6$	N/m
All tire damping	$D_{wf}, D_{wr}, D_{wtf}, D_{wtr}$	0	Ns/m
<b>— Mass properties (half-model) —</b>			
Truck sprung mass (half)	$m_c$	11,000	kg
Front unsprung mass (half, truck)	$m_{uf}$	250	kg
Rear unsprung mass (half, truck)	$m_{ur}$	750	kg
Trailer sprung mass (half)	$m_{ct}$	13,250	kg
Trailer front unsprung mass (half)	$m_{uft}$	500	kg
Trailer rear unsprung mass (half)	$m_{urt}$	500	kg
Drawbar mass (half)	$m_d$	125	kg
<b>— Geometry —</b>			
CG–front axle (truck)	$l_f$	4.528	m
CG–rear axle (truck)	$l_r$	0.942	m
CG–front axle (trailer)	$l_{ft}$	3.965	m
CG–rear axle (trailer)	$l_{rt}$	2.985	m

Continued on next page

**Table 2 (continued)**

<b>Parameter</b>	<b>Symbol</b>	<b>Value</b>	<b>Unit</b>
Distance CG <sub>truck</sub> –drawbar joint	$a_1$	3.867	m
Distance CG <sub>trailer</sub> –drawbar joint	$a_2$	5.565	m
Drawbar front offset	$l_{fd}$	1.1025	m
Drawbar rear offset	$l_{rd}$	0.8525	m
<b>— Inertia (computed in script) —</b>			
Truck pitch inertia	$I_y = \frac{m_c(l_f^2+l_r^2)}{2}$	—	kg·m <sup>2</sup>
Trailer pitch inertia	$I_{yt} = \frac{m_{ct}(l_{ft}^2+l_{rt}^2)}{2}$	—	kg·m <sup>2</sup>
Drawbar pitch inertia	$I_{yd} = \frac{m_d(l_{fd}^2+l_{rd}^2)}{2}$	—	kg·m <sup>2</sup>
<b>— Road parameters —</b>			
Forward speed (sweep)	$V_x$	5, 10, 15, 20, 25	m/s
Road wavelength	$\lambda$	10	m
Angular frequency	$\omega = 2\pi V_x/\lambda$	—	rad/s
Axle longitudinal positions	$s_1, s_2, s_3, s_4$	1.365, 6.835, 13.315, 20.265	m
Axle delay times	$t_i = s_i/V_x$	—	s

## B State-Space model

### B.1 Equations of Motion

#### B.1.1 Sprung Mass (Truck and Trailer)

Truck Heave:

$$\begin{aligned}
 m_1\ddot{y} = & -C_{sf}(y - l_f\phi_1 - y_1) - D_{sf}(\dot{y} - l_f\dot{\phi}_1 - \dot{y}_1) \\
 & - C_{sr}(y + l_r\phi_1 - y_2) - D_{sr}(\dot{y} + l_r\dot{\phi}_1 - \dot{y}_2) \\
 & - C_{sd}(y + a_1\phi_1 - w + l_{fd}\phi_3) - D_{sd}(\dot{y} + a_1\dot{\phi}_1 - \dot{w} + l_{fd}\dot{\phi}_3)
 \end{aligned} \tag{7}$$

Trailer Heave:

$$\begin{aligned}
 m_2\ddot{Y} = & -C_{sft}(Y - l_{ft}\phi_2 - y_3) - D_{sft}(\dot{Y} - l_{ft}\dot{\phi}_2 - \dot{y}_3) \\
 & - C_{srt}(Y + l_{rt}\phi_2 - y_4) - D_{srt}(\dot{Y} + l_{rt}\dot{\phi}_2 - \dot{y}_4) \\
 & - C_{sd}(Y - a_2\phi_2 - w - l_{rd}\phi_3) - D_{sd}(\dot{Y} - a_2\dot{\phi}_2 - \dot{w} - l_{rd}\dot{\phi}_3)
 \end{aligned} \tag{8}$$

Truck Pitch:

$$\begin{aligned}
 I_y\ddot{\phi}_1 = & -C_{sf}(y_1 + l_f\phi_1 - y)l_f - D_{sf}(\dot{y}_1 + l_f\dot{\phi}_1 - \dot{y})l_f \\
 & + C_{sr}(y_2 - y - l_r\phi_1)l_r + D_{sr}(\dot{y}_2 - \dot{y} - l_r\dot{\phi}_1)l_r \\
 & - C_{sd}(y + a_1\phi_1 - w + l_{fd}\phi_3)a_1 \\
 & - D_{sd}(\dot{y} + a_1\dot{\phi}_1 - \dot{w} + l_{fd}\dot{\phi}_3)a_1
 \end{aligned} \tag{9}$$

Trailer Pitch:

$$\begin{aligned}
 I_{yt}\ddot{\phi}_2 = & -C_{sft}(y_3 + l_{ft}\phi_2 - Y)l_{ft} - D_{sft}(\dot{y}_3 + l_{ft}\dot{\phi}_2 - \dot{Y})l_{ft} \\
 & + C_{srt}(y_4 - Y - l_{rt}\phi_2)l_{rt} + D_{srt}(\dot{y}_4 - \dot{Y} - l_{rt}\dot{\phi}_2)l_{rt} \\
 & + C_{sd}(Y - a_2\phi_2 - w - l_{rd}\phi_3)a_2 \\
 & + D_{sd}(\dot{Y} - a_2\dot{\phi}_2 - \dot{w} - l_{rd}\dot{\phi}_3)a_2
 \end{aligned} \tag{10}$$

#### B.1.2 Un-sprung Masses (Truck and Trailer)

Truck front axle:

$$m_{u1}\ddot{y}_1 = C_{sf}(y - l_f\phi_1 - y_1) + D_{sf}(\dot{y} - l_f\dot{\phi}_1 - \dot{y}_1) + C_{wf}(z_1 - y_1) \tag{11}$$

Truck rear axle

$$m_{u2}\ddot{y}_2 = C_{sr}(y + l_r\phi_1 - y_2) + D_{sr}(\dot{y} + l_r\dot{\phi}_1 - \dot{y}_2) + C_{wr}(z_2 - y_2) \tag{12}$$

Trailer front axle:

$$m_{u3}\ddot{y}_3 = C_{sft}(Y - l_{ft}\phi_2 - y_3) + D_{sft}(\dot{Y} - l_{ft}\dot{\phi}_2 - \dot{y}_3) + C_{wft}(z_3 - y_3) \tag{13}$$

Trailer rear axle:

$$m_{u4}\ddot{y}_4 = C_{srt}(Y + l_{rt}\phi_2 - y_4) + D_{srt}(\dot{Y} + l_{rt}\dot{\phi}_2 - \dot{y}_4) + C_{wrt}(z_4 - y_4) \tag{14}$$

### B.1.3 Drawbar Dynamics

**Kinematics:**

$$w_f = y + a_1\phi_1 - (w - l_{fd}\phi_3), \quad w_r = Y - a_2\phi_2 - (w - l_{rd}\phi_3) \quad (15)$$

**Heave:**

$$\begin{aligned} m_d\ddot{w} = & C_{sd_f}(y + a_1\phi_1 - w + l_{fd}\phi_3) + D_{sd_f}(\dot{y} + a_1\dot{\phi}_1 - \dot{w} + l_{fd}\dot{\phi}_3) \\ & + C_{sd_r}(Y - a_2\phi_2 - w - l_{rd}\phi_3) + D_{sd_r}(\dot{Y} - a_2\dot{\phi}_2 - \dot{w} - l_{rd}\dot{\phi}_3) \end{aligned} \quad (16)$$

**Pitch:**

$$\begin{aligned} I_{yd}\ddot{\phi}_3 = & C_{sd_r}l_{rd}(Y - a_2\phi_2 - w - l_{rd}\phi_3) + D_{sd_r}l_{rd}(\dot{Y} - a_2\dot{\phi}_2 - \dot{w} - l_{rd}\dot{\phi}_3) \\ & - C_{sd_f}l_{fd}(y + a_1\phi_1 - w + l_{fd}\phi_3) \\ & - D_{sd_f}l_{fd}(\dot{y} + a_1\dot{\phi}_1 - \dot{w} + l_{fd}\dot{\phi}_3) \end{aligned} \quad (17)$$

## B.2 Matlab script

```
1 %% Before running the code, put a breakpoint at line 486 and
   perform the sweep first
2 % clear all
3 % close all
4 clc
5 %% Variable and Parameter Definition
6 syms y Y w y1 y2 y3 y4 y_dot Y_dot w_dot y1_dot y2_dot y3_dot
   y4_dot y_ddot Y_ddot w_ddot y1_ddot y2_ddot y3_ddot
   y4_ddot
7 syms phi1 phi1_dot phi1_ddot phi2 phi2_dot phi2_ddot phi3
   phi3_dot phi3_ddot z1 z2 z3 z4 z1_dot z2_dot z3_dot z4_dot
8
9 % Truck Parameters
10 Csf = 240000/2; % Spring Stiffness of Truck (Front)
11 Dsf = 12000/2; % Damping Coefficient of Truck (Front)
12 Csr = 3*300000/2; % Spring Stiffness of Truck (Rear)
13 Dsr = 3*12000/2; % Damping Coefficient of Truck (Rear)
14
15 % Trailer Parameters
16 Csft = 2*240000/2; % Spring Stiffness of Trailer (Front)
17 Dsft = 2*13000/2; % Damping Coefficient of Trailer (Front)
18 Csrt = 3*300000/2; % Spring Stiffness of Trailer (Rear)
19 Dsrt = 3*13000/2; % Damping Coefficient of Trailer (Rear)
20
21 % Tire Parameters
22 Cwr = 3*850000; % Radial Stiffness of Truck tire (Rear)
23 Dwr = 0; % Damping Coefficient of Truck tire (Rear)
24 Cwtr = 3*850000; % Radial Stiffness of Trailer tire (Rear)
25 Dwtr = 0; % Damping Coefficient of Trailer tire (
   Rear)
26 Cwf = 850000; % Radial Stiffness of Truck tire (Front)
27 Dwf = 0; % Damping Coefficient of Truck tire (Front
   )
28 Cwtf = 2*850000; % Radial Stiffness of Trailer tire (Front)
29 Dwtf = 0; % Damping Coefficient of Trailer tire (
   Front)
30
31 % Dimensions
32 lf = 4.528; % Distance from COG to Front axle (Truck)
33 lr = 0.942; % Distance from COG to Rear axle (Truck)
34 lft = 3.965; % Distance from COG to Front axle (Trailer)
35 lrt = 2.985; % Distance from COG to Rear axle (Trailer)
36 a1 = 3.867; % Distance from Truck's COG to Drawbar's
   articulation point
37 a2 = 5.565; % Distance from Trailer's COG to Drawbar's
   articulation point
38
39 % Masses (full-load nominal, will be overwritten in sweep)
```

```

40 m_c    = 30000/2;    % Truck = Kerb Weight (12000) + Load
    (20000)
41 m_uf   = 500/2;    % Unsprung mass at Front (Truck)
42 m_ur   = 1500/2;   % Unsprung mass at Rear (Truck)
43 m_ct   = 40000/2;  % Trailer = Kerb Weight (11000) + Load
    (31000)
44 m_uft  = 1000/2;   % Unsprung mass at Front (Trailer)
45 m_urt  = 1000/2;   % Unsprung mass at Rear (Trailer)
46
47 % Drawbar Parameters
48 m_d    = 250/2;    % Mass of the Drawbar
49 lfd    = 1.1025;   % Distance from COG of drawbar to the front
    Articulation point
50 lrd    = 0.8525;   % Distance from COG of drawbar to the rear
    Articulation point
51 Csd    = 6000000;  % Spring Stiffness of the Drawbar
52 Dsd    = 50000;    % Damping Coefficient of the Drawbar
53
54 alpha  = 1;
55 Beta   = 1;
56 g      = 9.81;
57
58 % Inertias (for initial full-load case; will be recomputed in
    sweep)
59 Iy     = m_c*(lf^2 + lr^2)/2;    % Truck
60 Iyt    = m_ct*(lft^2 + lrt^2)/2; % Trailer
61 Iyd    = m_d*(lfd^2 + lrd^2)/2; % Drawbar
62
63 % Disturbance Start time
64 tref_start = 0.5; % [Secs] Used in Simulink, Change here to
    reflect in Simulink
65
66 % Bridge Length
67 L = 15; % [m]
68
69 %%
-----
70 %% Function to compute Settling Time
71 %%
-----
72
73 % Settling time function
74
75 function Ts = settling_time(t, y)
76
77     tol = 0.05;    % 5 % band
78
79     y_final = y(end); % steady-state approx

```

```

80     band_hi = y_final * (1 + tol);
81     band_lo = y_final * (1 - tol);
82
83     idx = find(y < band_lo | y > band_hi); % indices outside
      band
84
85     if isempty(idx)
86         Ts = 0; % already settled
87     else
88         Ts = t(idx(end)); % last time outside band
89     end
90 end
91
92 %%
-----
93 %% Load / velocity sweep and plots
94 %%
-----
95
96 % Mass decomposition from your comments
97 kerbTruck    = 12000;  loadTruck    = 20000;
98 kerbTrailer  = 11000;  loadTrailer  = 31000;
99
100 % Load cases & labels
101 loadFactors  = [1.0, 0.5, 0.0];
102 loadNames    = {'FullLoad', 'HalfLoad', 'NoLoad'};
103
104 % Velocities [m/s]
105 Vx_list     = [5 10 15 20 25];
106
107 % Folder for all figures
108 figRoot     = 'Figures';
109 if ~exist(figRoot, 'dir'); mkdir(figRoot); end
110
111 % RESULTS STRUCTURE
112 Results     = struct();
113
114 for iLoad   = 1:numel(loadFactors)
115     fLoad    = loadFactors(iLoad);
116     loadStr  = loadNames{iLoad};
117
118     % Store per-load-case struct
119     Results.(loadStr) = struct();
120
121     % Update sprung masses
122     m_c     = (kerbTruck + fLoad*loadTruck) / 2;
123     m_ct    = (kerbTrailer + fLoad*loadTrailer) / 2;
124

```

```

125 % Recompute inertias
126 Iy = m_c *(lf^2 + lr^2 )/2;
127 Iyt = m_ct*(lft^2 + lrt^2)/2;
128 Iyd = m_d *(lfd^2 + lrd^2)/2;
129
130 fprintf('\n=== Load case: %s (factor %.2f), m_c=%.1f,
      m_ct=%.1f ===\n', ...
131         loadStr, fLoad, m_c, m_ct);
132
133 for iV = 1:numel(Vx_list)
134     Vx = Vx_list(iV);
135
136     %% Rebuild A,B,C,D for this mass/inertia
137
138     M = [m_c 0 0 0 0 0 0 0 0 0 ;
139         0 m_uf 0 0 0 0 0 0 0 0 ;
140         0 0 m_ur 0 0 0 0 0 0 0 ;
141         0 0 0 Iy 0 0 0 0 0 0 ;
142         0 0 0 0 m_ct 0 0 0 0 0 ;
143         0 0 0 0 0 m_uft 0 0 0 0 ;
144         0 0 0 0 0 0 m_urt 0 0 0 ;
145         0 0 0 0 0 0 0 Iyt 0 0 ;
146         0 0 0 0 0 0 0 0 m_d 0 ;
147         0 0 0 0 0 0 0 0 0 Iyd];
148
149     C = [-(Csf+Csr+Csd) Csf Csr (-Csr*lr+Csf*lf-Csd*a1) 0 0 0
          0 Csd -Csd*lfd;
150     Csf -(Csf+Cwf) 0 -Csf*lf 0 0 0 0 0 0;
151     Csr 0 -(Csr+Cwr) Csr*lr 0 0 0 0 0 0;
152     (-Csr*lr+Csf*lf-Csd*a1) -Csf*lf Csr*lr -(Csr*lr^2+Csf*lf
          ^2+Csd*a1^2) 0 0 0 0 Csd*a1 -Csd*lfd*a1;
153     0 0 0 0 -(Csft+Csrt+Csd) Csft Csrt (-Csrt*lrt+Csft*lft+
          Csd*a2) Csd Csd*lrd ;
154     0 0 0 0 Csft -(Csft+Cwtf) 0 -Csft*lft 0 0;
155     0 0 0 0 Csrt 0 -(Csrt+Cwtr) Csrt*lrt 0 0;
156     0 0 0 0 (-Csrt*lrt+Csft*lft+Csd*a2) -Csft*lft Csrt*lrt -(
          Csrt*lrt^2+Csft*lft^2+Csd*a2^2) -Csd*a2 -Csd*lrd*a2;
157     Csd 0 0 (Csd*a1) Csd 0 0 (-Csd*a2) -(Csd+Csd) (Csd*lfd-
          Csd*lrd);
158     -Csd*lfd 0 0 (-Csd*lfd*a1) Csd*lrd 0 0 (-Csd*lrd*a2) (-
          Csd*lrd+Csd*lfd) -(Csd*lfd^2+Csd*lrd^2) ];
159
160     K = [-(Dsf+Dsr+Dsd) Dsf Dsr (-Dsr*lr+Dsf*lf-Dsd*a1) 0 0 0
          0 Dsd -Dsd*lfd;
161     Dsf -Dsf 0 -Dsf*lf 0 0 0 0 0 0;
162     Dsr 0 -Dsr Dsr*lr 0 0 0 0 0 0;
163     (-Dsr*lr+Dsf*lf-Dsd*a1) -Dsf*lf Dsr*lr -(Dsr*lr^2+Dsf*lf
          ^2+Dsd*a1^2) 0 0 0 0 Dsd*a1 -Dsd*lfd*a1;
164     0 0 0 0 -(Dsft+Dsrt+Dsd) Dsft Dsrt (-Dsrt*lrt+Dsft*lft+
          Dsd*a2) Dsd Dsd*lrd;

```

```

165 0 0 0 0 Dsft -Dsft 0 -Dsft*lft 0 0;
166 0 0 0 0 Dsrt 0 -Dsrt Dsrt*lrt 0 0;
167 0 0 0 0 (-Dsrt*lrt+Dsft*lft+Dsd*a2) -Dsft*lft Dsrt*lrt -(
    Dsrt*lrt^2+Dsft*lft^2+Dsd*a2^2) -Dsd*a2 -Dsd*lrd*a2;
168 Dsd 0 0 (Dsd*a1) Dsd 0 0 (-Dsd*a2) -(Dsd+Dsd) (Dsd*lfd-
    Dsd*lrd);
169 -Dsd*lfd 0 0 (-Dsd*lfd*a1) Dsd*lrd 0 0 (-Dsd*lrd*a2) (-
    Dsd*lrd+Dsd*lfd) -(Dsd*lfd^2+Dsd*lrd^2)];
170
171 F = [m_c*g; m_uf*g; m_ur*g; 0; m_ct*g; m_uft*g; m_urt*g;
    0; m_d*g; 0];
172
173 q0 = C\F;
174
175 x0 = [q0; zeros(size(q0))];
176
177 A = [zeros(10) eye(10);
178 M\C M\K];
179
180 B = [0 0 0 0;
181 0 0 0 0;
182 0 0 0 0;
183 0 0 0 0;
184 0 0 0 0;
185 0 0 0 0;
186 0 0 0 0;
187 0 0 0 0;
188 0 0 0 0;
189 0 0 0 0;
190 0 0 0 0;
191 Cwf/m_uf 0 0 0;
192 0 Cwr/m_ur 0 0;
193 0 0 0 0;
194 0 0 0 0;
195 0 0 Cwtf/m_uft 0;
196 0 0 0 Cwtr/m_urt;
197 0 0 0 0;
198 0 0 0 0;
199 0 0 0 0];
200
201
202 C_ss = eye(20);
203
204 D = zeros(20,4);
205
206 U0 = zeros(size(x0));
207
208
209 %% Road parameters for this Vx
210

```

```

211     s1 = 1.365;
212     s2 = 5.47 + 1.365;
213     s3 = 11.95 + 1.365;
214     s4 = 18.9 + 1.365;
215     t1 = s1/Vx;
216     t2 = s2/Vx;
217     t3 = s3/Vx;
218     t4 = s4/Vx;
219
220     % Reference time for each axle group, time instant
       at which it hits the bump
221
222     tref_1 = tref_start + t1;
223     tref_2 = tref_start + t2;
224     tref_3 = tref_start + t3;
225     tref_4 = tref_start + t4;
226
227
228     fprintf(' -> Simulating Vx = %2d m/s\n', Vx);
229
230     % Run Simulink model (writes out to base workspace
       )
231
232     sim('Truck_staticEq_step.slx'); % Truck_model_bump
       or Truck_model_step
233
234     % Now out exists exactly like in your original
       script.
235
236     % Compute forces & deflections and save figures for
       this case
237     modelTag = 'step'; % step or 'bump'
238
239     % Compute forces & deflections and save figures for
       this case
240     caseTag = sprintf('%s_V%02d_%s', loadStr, Vx,
       modelTag);
241     caseFolder = fullfile(figRoot, caseTag);
242     if ~exist(caseFolder, 'dir'); mkdir(caseFolder); end
243
244     % Tractor tire forces
245     Ftractor_Rear = Cwr * (ans.y2.Data - ans.z2.Data);
       %- m_c*lf*g/(lr+lf) - m_ur*g;
246     Ftractor_Front = Cwf * (ans.y1.Data - ans.z1.Data);
       %- m_c*lr*g/(lr+lf) - m_uf*g;
247     Fstat_tractor_Rear = m_c*lf*g/(lr+lf) + m_ur*g;
248     Fstat_tractor_Front = m_c*lr*g/(lr+lf) + m_uf*g;
249     % Peak Force value
250     FPeak_tractor_Rear = max(abs(Ftractor_Rear));
251     FPeak_tractor_Front = max(abs(Ftractor_Front));

```

```

252     % Force Amplification
253     AF_tractor_Rear = FPeak_tractor_Rear/
        Fstat_tractor_Rear;
254     AF_tractor_Front = FPeak_tractor_Front/
        Fstat_tractor_Front;
255     % Settling Time
256     t = ans.tout;
257     Ts_Tractor_Front = settling_time(t, -Ftractor_Front)
        ;
258     Ts_Tractor_Rear = settling_time(t, -Ftractor_Rear)
        ;
259     % Force in Spatial Domain
260     F1 = Ftractor_Front ;
261     F2 = Ftractor_Rear ;
262     x1 = Vx*(t-tref_1);
263     x2 = Vx*(t-tref_2);
264
265     % Extracting forces only along the bridge
266
267     I1 = find(x1 >= 0 & x1 <= L);
268     F1_bridge = F1(I1);
269     x1_bridge = x1(I1);
270
271
272     I2 = find(x2 >= 0 & x2 <= L);
273     F2_bridge = F2(I2);
274     x2_bridge = x2(I2);
275
276
277
278
279     f1 = figure('Visible','off');
280     plot(ans.tout,Ftractor_Front,'r-'); hold on;
281     plot(ans.tout,Ftractor_Rear , 'b--');
282     title(sprintf('Tractor Tire Forces (%s)', caseTag), '
        Interpreter','none');
283     xlabel('Time [s]'); ylabel('Force [N]');
284     legend('Front','Rear','Location','best');
285     grid on;
286     exportgraphics(f1, fullfile(caseFolder,'TractorForces
        .png'));
287     close(f1);
288
289     % Trailer tire forces
290     Ftrailer_Rear = Cwtr * (ans.y4.Data - ans.z4.Data);
        %- m_ct*lft*g/(lrt+lft) - m_urt*g;
291     Ftrailer_Front = Cwtf * (ans.y3.Data - ans.z3.Data);
        %- m_ct*lrt*g/(lrt+lft) - m_uft*g;
292     Fstat_trailer_Rear = m_ct*lft*g/(lrt+lft) + m_urt*g;

```

```

293     Fstat_trailer_Front = m_ct*lrt*g/(lrt+lft) + m_uft*g
      ;
294     % Peak Force value
295     FPeak_trailer_Rear = max(abs(Ftrailer_Rear));
296     FPeak_trailer_Front = max(abs(Ftrailer_Front));
297     % Force Amplification
298     AF_trailer_Rear = FPeak_trailer_Rear/
      Fstat_trailer_Rear;
299     AF_trailer_Front = FPeak_trailer_Front/
      Fstat_trailer_Front;
300     % Settling Time
301     Ts_Trailer_Front = settling_time(t, -Ftrailer_Front)
      ;
302     Ts_Trailer_Rear = settling_time(t, -Ftrailer_Rear)
      ;
303     % Force in Spatial Domain
304     F3 = Ftrailer_Front;
305     F4 = Ftrailer_Rear;
306     x3 = Vx*(t-tref_3);
307     x4 = Vx*(t-tref_4);
308
309     % Extracting forces only along the bridge
310
311     I3 = find(x3 >= 0 & x3 <= L);
312     F3_bridge = F3(I3);
313     x3_bridge = x3(I3);
314
315
316     I4 = find(x4 >= 0 & x4 <= L);
317     F4_bridge = F4(I4);
318     x4_bridge = x4(I4);
319
320
321
322
323     f2 = figure('Visible','off');
324     plot(ans.tout,Ftrailer_Front,'r-'); hold on;
325     plot(ans.tout,Ftrailer_Rear , 'b--');
326     title(sprintf('Trailer Tire Forces (%s)', caseTag), '
      Interpreter','none');
327     xlabel('Time [s]'); ylabel('Force [N]');
328     legend('Front','Rear','Location','best');
329     grid on;
330     exportgraphics(f2, fullfile(caseFolder,'TrailerForces
      .png'));
331     close(f2);
332
333
334     % STORE ALL RESULTS

```

335  
336  
337  
338  
339  
340  
341  
342  
343  
344  
345  
346  
347  
348  
349  
350  
351  
352  
353  
354  
355  
356  
357  
358  
359  
360  
361  
362

```
%  
=====
```

```
speedTag = sprintf('V%02d', Vx);  
Results.(loadStr).(speedTag).folder = caseFolder;  
Results.(loadStr).(speedTag).Fstat_tractor_Front =  
    Fstat_tractor_Front;  
Results.(loadStr).(speedTag).Fstat_tractor_Rear =  
    Fstat_tractor_Rear;  
Results.(loadStr).(speedTag).Fpeak_tractor_Front =  
    FPeak_tractor_Front;  
Results.(loadStr).(speedTag).Fpeak_tractor_Rear =  
    FPeak_tractor_Rear;  
Results.(loadStr).(speedTag).AF_tractor_Front =  
    AF_tractor_Front;  
Results.(loadStr).(speedTag).AF_tractor_Rear =  
    AF_tractor_Rear;  
Results.(loadStr).(speedTag).Fstat_trailer_Front =  
    Fstat_trailer_Front;  
Results.(loadStr).(speedTag).Fstat_trailer_Rear =  
    Fstat_trailer_Rear;  
Results.(loadStr).(speedTag).Fpeak_trailer_Front =  
    FPeak_trailer_Front;  
Results.(loadStr).(speedTag).Fpeak_trailer_Rear =  
    FPeak_trailer_Rear;  
Results.(loadStr).(speedTag).AF_trailer_Front =  
    AF_trailer_Front;  
Results.(loadStr).(speedTag).AF_trailer_Rear =  
    AF_trailer_Rear;  
Results.(loadStr).(speedTag).SettlingTime_Tractor_F  
    = Ts_Tractor_Front;  
Results.(loadStr).(speedTag).SettlingTime_Tractor_R  
    = Ts_Tractor_Rear;  
Results.(loadStr).(speedTag).SettlingTime_Trailer_F  
    = Ts_Trailer_Front;  
Results.(loadStr).(speedTag).SettlingTime_Trailer_R  
    = Ts_Trailer_Rear;  
  
% Force Vector over the Bridge span  
Results.(loadStr).(speedTag).Faxle1_Bridge =  
    F1_bridge;  
Results.(loadStr).(speedTag).Faxle2_Bridge =  
    F2_bridge;  
Results.(loadStr).(speedTag).Faxle3_Bridge =  
    F3_bridge;
```

```

363 Results.(loadStr).(speedTag).Faxle4_Bridge =
      F4_bridge;
364
365 % Time instant when the axle group comes in contact
      with the bridge
366 Results.(loadStr).(speedTag).Time_axle1_Bridge =
      tref_1;
367 Results.(loadStr).(speedTag).Time_axle2_Bridge =
      tref_2;
368 Results.(loadStr).(speedTag).Time_axle3_Bridge =
      tref_3;
369 Results.(loadStr).(speedTag).Time_axle4_Bridge =
      tref_4;
370
371
372
373 % Truck deflection
374 f3 = figure('Visible','off');
375 plot(ans.tout,ans.y.Data,'r-','LineWidth',1.2);
376 title(sprintf('Truck Sprung Mass Deflection (%s)',
      caseTag), 'Interpreter','none');
377 xlabel('Time [s]'); ylabel('Deflection [m]');
378 grid on;
379 exportgraphics(f3, fullfile(caseFolder,'
      TruckDeflection.png'));
380 close(f3);
381
382 % Trailer deflection
383 f4 = figure('Visible','off');
384 plot(ans.tout,ans.Y.Data,'b-','LineWidth',1.2);
385 title(sprintf('Trailer Sprung Mass Deflection (%s)',
      caseTag), 'Interpreter','none');
386 xlabel('Time [s]'); ylabel('Deflection [m]');
387 grid on;
388 exportgraphics(f4, fullfile(caseFolder,'
      TrailerDeflection.png'));
389 close(f4);
390
391 % Drawbar deflection
392 f5 = figure('Visible','off');
393 plot(ans.tout,ans.W.Data,'k-','LineWidth',1.2);
394 title(sprintf('Drawbar Deflection (%s)', caseTag), '
      Interpreter','none');
395 xlabel('Time [s]'); ylabel('Deflection [m]');
396 grid on;
397 exportgraphics(f5, fullfile(caseFolder,'
      DrawbarDeflection.png'));
398 close(f5);
399
400 % Force Spatial Truck Front

```

```

401     f6 = figure('Visible','off');
402     plot(x1_bridge,F1_bridge,'r-','LineWidth',1.2);
403     yline(-Fstat_tractor_Front,'-','Static Load');
404     title(sprintf('Force along the Bridge span (%s)',
405                 caseTag), 'Interpreter','none');
406     xlabel('Distance [m]'); ylabel('Force [N]');
407     legend('Total Force','Location','east')
408     grid on;
409     exportgraphics(f6, fullfile(caseFolder,'Truck F Force
410                               along the Bridge span.png'));
411     close(f6);
412
413     % Force Spatial Truck Rear
414     f7 = figure('Visible','off');
415     plot(x2_bridge,F2_bridge,'r-','LineWidth',1.2);
416     yline(-Fstat_tractor_Rear,'-','Static Load');
417     title(sprintf('Force along the Bridge span (%s)',
418                 caseTag), 'Interpreter','none');
419     xlabel('Distance [m]'); ylabel('Force [N]');
420     legend('Total Force','Location','east')
421     grid on;
422     exportgraphics(f7, fullfile(caseFolder,'Truck R Force
423                               along the Bridge span.png'));
424     close(f7);
425
426     % Force Spatial Trailer Front
427     f8 = figure('Visible','off');
428     plot(x3_bridge,F3_bridge,'r-','LineWidth',1.2);
429     yline(-Fstat_trailer_Front,'-','Static Load');
430     title(sprintf('Force along the Bridge span (%s)',
431                 caseTag), 'Interpreter','none');
432     xlabel('Distance [m]'); ylabel('Force [N]');
433     legend('Total Force','Location','east')
434     grid on;
435     exportgraphics(f8, fullfile(caseFolder,'Trailer F
436                               Force along the Bridge span.png'));
437     close(f8);
438
439     % Force Spatial Trailer Rear
440     f9 = figure('Visible','off');
441     plot(x4_bridge,F4_bridge,'r-','LineWidth',1.2);
442     yline(-Fstat_trailer_Rear,'-','Static Load');
443     title(sprintf('Force along the Bridge span (%s)',
444                 caseTag), 'Interpreter','none');
445     xlabel('Distance [m]'); ylabel('Force [N]');
446     legend('Total Force','Location','east')
447     grid on;

```

```

443     exportgraphics(f9, fullfile(caseFolder, 'Trailer R
      Force along the Bridge span.png'));
444 close(f9);
445
446
447
448     %% Frequency Analysis
449     % fs = 20;
450     % t = ans.tout;
451     % freq = 0:fs/length(t):fs-1/fs;
452     % xn = Ftractor_Front;
453     % N = length(xn); % Number of samples
454     % xk = abs(fft(xn))/N; % Two-sided amplitude
455     % xk = xk(1:(N+1)/2); % One-sided
456     % xk(2:end-1) = 2*xk(2:end-1); % Double values
      except for DC and Nyquist
457     % f6 = figure('Visible','off');
458     % periodogram(Ftractor_Front, hamming(length(
      Ftractor_Front)), length(Ftractor_Front), fs, 'psd
      ')
459     % title(sprintf('Power Frequency spectrum (%s)',
      caseTag), 'Interpreter','none');
460     % xlabel('Frequency [s]'); ylabel('Power [dB]');
461     % grid on;
462     % exportgraphics(f6, fullfile(caseFolder, '
      FrequencySpectrumTractorFront.png'));
463     % close(f6);
464     %
465     %
466     % f7 = figure('Visible','off');
467     % periodogram(Ftractor_Rear, hamming(length(
      Ftractor_Rear)), length(Ftractor_Rear), fs, 'psd')
468     % title(sprintf('Power Frequency spectrum (%s)',
      caseTag), 'Interpreter','none');
469     % xlabel('Frequency [s]'); ylabel('Power [dB]');
470     % grid on;
471     % exportgraphics(f7, fullfile(caseFolder, '
      FrequencySpectrumTractorRear.png'));
472     % close(f7);
473
474
475     end
476 end
477
478 fprintf('\nSweep complete.\n');
479
480
481
482 %% Peak Forces and Force Amplification
483

```

```

484
485
486 plotFolder = 'SummaryPlots';
487 if ~exist(plotFolder,'dir'); mkdir(plotFolder); end
488
489 loadCases = {'FullLoad','HalfLoad','NoLoad'};
490 speedList = [5 10 15 20 25];
491 speedTags = arrayfun(@(v) sprintf('V%02d',v), speedList, '
    UniformOutput',false);
492
493 % Helper extractor
494 getField = @(S,field) arrayfun(@(v) S.(v{1}).(field),
    speedTags);
495
496 colors = {'r','b','k'}; % Front / Rear
497 styles = {'-','-',':'}; % Full Load / No Load
498
499
500 % ===== TRACTOR PEAK FORCE
    =====
501 figure; hold on; grid on;
502
503 for iLoad = 1:3
504     LC = loadCases{iLoad};
505     style = styles{iLoad};
506
507     % Front
508     PF_front = getField(Results.(LC),'Fpeak_tractor_Front');
509     plot(speedList, PF_front, [colors{1} style 'o'], ...
510         'LineWidth',1.5, 'DisplayName',[LC ' Front']);
511
512     % Rear
513     PF_rear = getField(Results.(LC),'Fpeak_tractor_Rear');
514     plot(speedList, PF_rear, [colors{2} style 'o'], ...
515         'LineWidth',1.5, 'DisplayName',[LC ' Rear']);
516 end
517
518 xlabel('Velocity [m/s]');
519 ylabel('Peak Force [N]');
520 title('Tractor Peak Forces vs Velocity');
521 legend('Location','best');
522 exportgraphics(gcf, fullfile(plotFolder,'Tractor_PeakForces.
    png'), 'Resolution',300);
523 close(gcf);
524
525
526 % ===== TRAILER PEAK FORCE
    =====
527 figure; hold on; grid on;
528

```

```

529 for iLoad = 1:3
530     LC = loadCases{iLoad};
531     style = styles{iLoad};
532
533     PF_front = getField(Results.(LC),'Fpeak_trailer_Front');
534     PF_rear  = getField(Results.(LC),'Fpeak_trailer_Rear');
535
536     plot(speedList, PF_front, [colors{1} style 'o'], ...
537         'LineWidth',1.5,'DisplayName',[LC ' Front']);
538     plot(speedList, PF_rear, [colors{2} style 'o'], ...
539         'LineWidth',1.5,'DisplayName',[LC ' Rear']);
540 end
541
542 xlabel('Velocity [m/s]');
543 ylabel('Peak Force [N]');
544 title('Trailer Peak Forces vs Velocity');
545 legend('Location','best');
546 exportgraphics(gcf, fullfile(plotFolder,'Trailer_PeakForces.
547     png'), 'Resolution',300);
548 close(gcf);
549
550 % ===== TRACTOR AF =====
551 figure; hold on; grid on;
552
553 for iLoad = 1:3
554     LC = loadCases{iLoad};
555     style = styles{iLoad};
556
557     AF_front = getField(Results.(LC),'AF_tractor_Front');
558     AF_rear  = getField(Results.(LC),'AF_tractor_Rear');
559
560     plot(speedList, AF_front, [colors{1} style 'o'], ...
561         'LineWidth',1.5,'DisplayName',[LC ' Front']);
562     plot(speedList, AF_rear, [colors{2} style 'o'], ...
563         'LineWidth',1.5,'DisplayName',[LC ' Rear']);
564 end
565
566 xlabel('Velocity [m/s]');
567 ylabel('Amplification Factor [-]');
568 title('Tractor Amplification Factor vs Velocity');
569 legend('Location','best');
570 exportgraphics(gcf, fullfile(plotFolder,'Tractor_AF.png'), '
571     Resolution',300);
572 close(gcf);
573
574 % ===== TRAILER AF =====
575 figure; hold on; grid on;
576

```

```

577 for iLoad = 1:3
578     LC = loadCases{iLoad};
579     style = styles{iLoad};
580
581     AF_front = getField(Results.(LC),'AF_trailer_Front');
582     AF_rear  = getField(Results.(LC),'AF_trailer_Rear');
583
584     plot(speedList, AF_front, [colors{1} style 'o'], ...
585         'LineWidth',1.5,'DisplayName',[LC ' Front']);
586     plot(speedList, AF_rear,  [colors{2} style 'o'], ...
587         'LineWidth',1.5,'DisplayName',[LC ' Rear']);
588 end
589
590 xlabel('Velocity [m/s]');
591 ylabel('Amplification Factor [-]');
592 title('Trailer Amplification Factor vs Velocity');
593 legend('Location','best');
594 exportgraphics(gcf, fullfile(plotFolder,'Trailer_AF.png'), '
    Resolution',300);
595 close(gcf);
596
597
598 % ===== TRACTOR SETTLING TIME
    =====
599 figure;
600 hold on;
601 grid on;
602
603 for iLoad = 1:3
604     LC = loadCases{iLoad};
605     style = styles{iLoad};
606
607     ST_front = getField(Results.(LC),'SettlingTime_Tractor_F'
        );
608     ST_rear  = getField(Results.(LC),'SettlingTime_Tractor_R'
        );
609
610     plot(speedList, ST_front, [colors{1} style 'o'], ...
611         'LineWidth',1.5,'DisplayName',[LC ' Front']);
612     plot(speedList, ST_rear,  [colors{2} style 'o'], ...
613         'LineWidth',1.5,'DisplayName',[LC ' Rear']);
614 end
615
616 xlabel('Velocity [m/s]');
617 ylabel('Settling Time [Secs]');
618 title('Tractor Contact Force Settling Time vs Velocity');
619 legend('Location','best');
620 exportgraphics(gcf, fullfile(plotFolder,'Tractor_ST.png'), '
    Resolution',300);
621 close(gcf);

```

```

622 |
623 | % ===== TRAILER SETTling TIME
        | =====
624 | figure;
625 | hold on;
626 | grid on;
627 |
628 | for iLoad = 1:3
629 |     LC = loadCases{iLoad};
630 |     style = styles{iLoad};
631 |
632 |     ST_front = getField(Results.(LC),'SettlingTime_Trailer_F'
        |         );
633 |     ST_rear  = getField(Results.(LC),'SettlingTime_Trailer_R'
        |         );
634 |
635 |     plot(speedList, ST_front, [colors{1} style 'o'], ...
636 |         'LineWidth',1.5,'DisplayName',[LC ' Front']);
637 |     plot(speedList, ST_rear,  [colors{2} style 'o'], ...
638 |         'LineWidth',1.5,'DisplayName',[LC ' Rear']);
639 | end
640 |
641 | xlabel('Velocity [m/s]');
642 | ylabel('Settling Time [Secs]');
643 | title('Trailer Contact Force Settling Time vs Velocity');
644 | legend('Location','best');
645 | exportgraphics(gcf, fullfile(plotFolder,'Trailer_ST.png'), '
        |     Resolution',300);
646 | close(gcf);
647 |
648 | disp('Combined plots generated successfully!');

```



# D Load and Velocity Sweep

## D.1 CASE – 1: Speed Bump

The speed bump was modelled in time domain using Sine function, it is a function of Longitudinal Velocity ( $V_x$ ), see Table 3 and Figure 20.

Table 3: Dimensions and timing of the bump

Parameter	Value
Width	0.5 m
Height	0.1 m
Bump start time	0.5 s

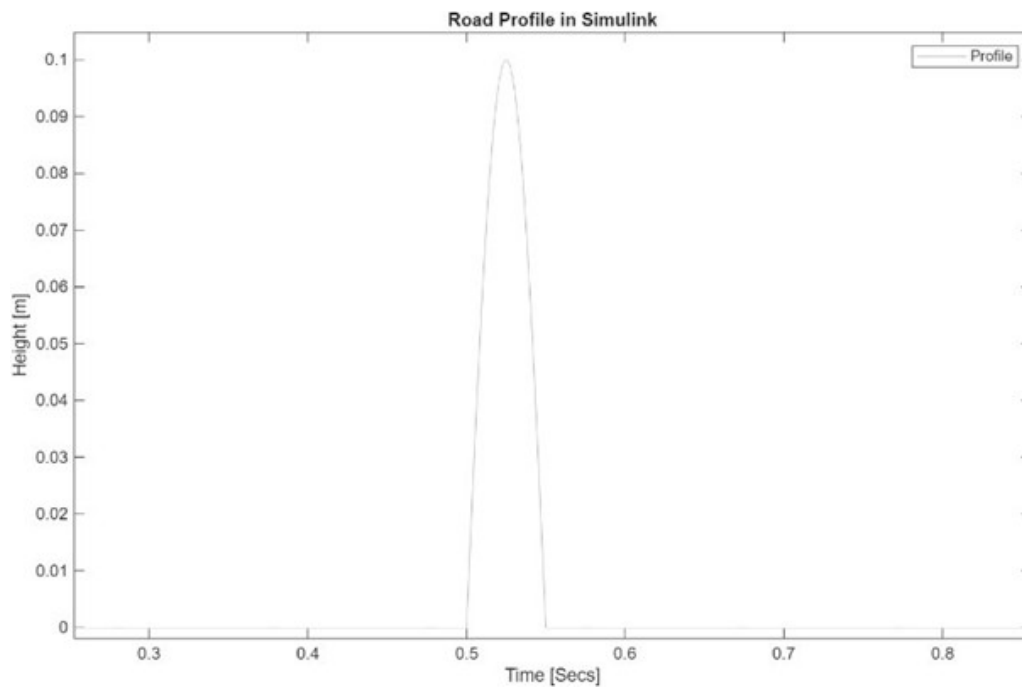
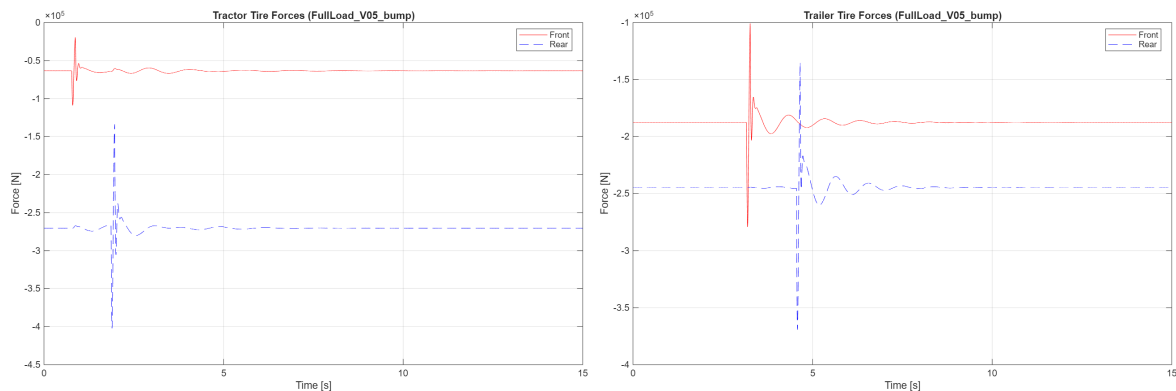


Figure 20: Bump Profile for  $V_x = 10$  m/s

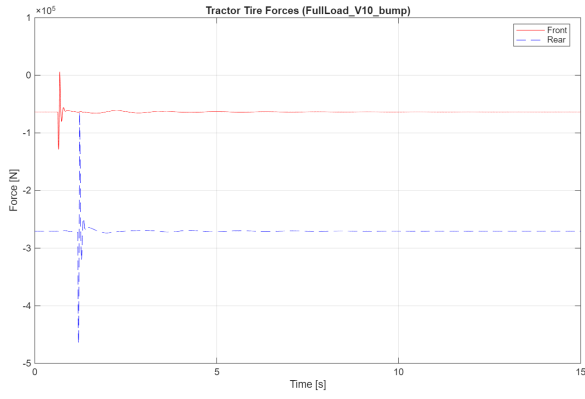
### Full load



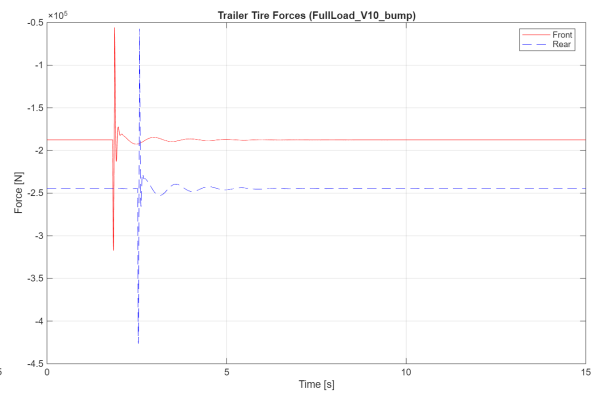
(a) Tractor,  $V = 5$  m/s

(b) Trailer,  $V = 5$  m/s

Figure 21: Tire contact forces for the FullLoad configuration over the bump profile at  $V = 5$  m/s.

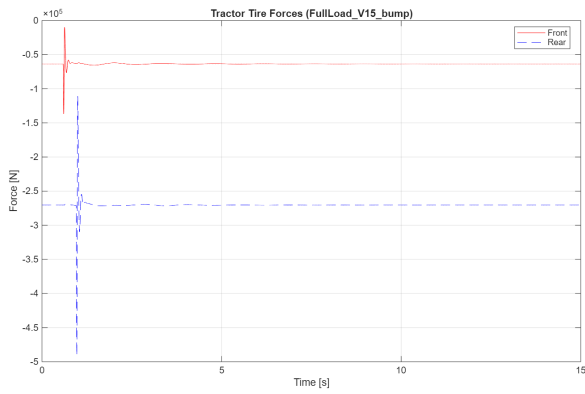


(a) Tractor,  $V = 10$  m/s

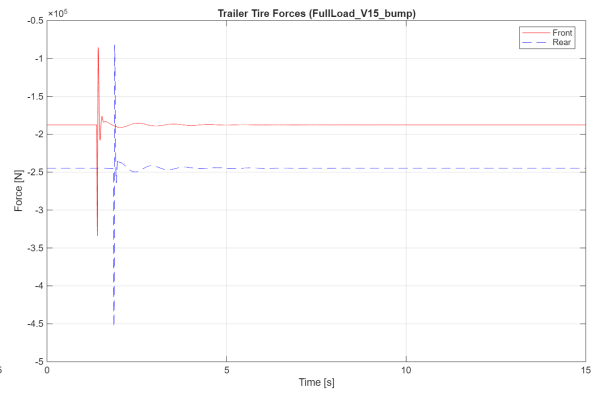


(b) Trailer,  $V = 10$  m/s

Figure 22: Tire contact forces for the FullLoad configuration over the bump profile at  $V = 10$  m/s.

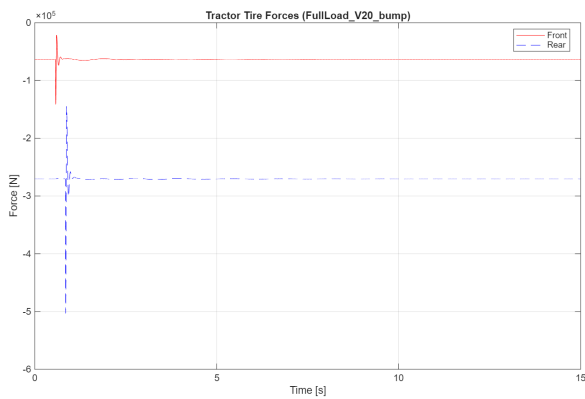


(a) Tractor,  $V = 15$  m/s

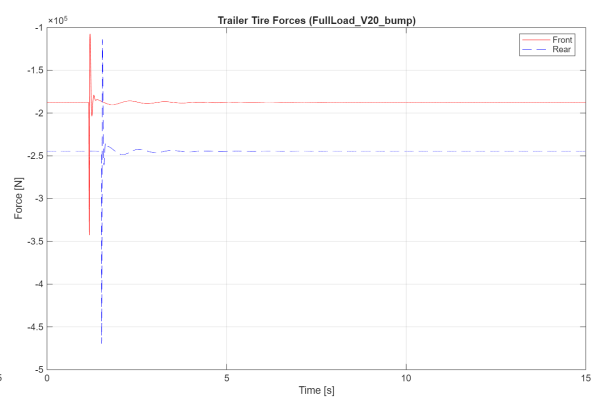


(b) Trailer,  $V = 15$  m/s

Figure 23: Tire contact forces for the FullLoad configuration over the bump profile at  $V = 15$  m/s.

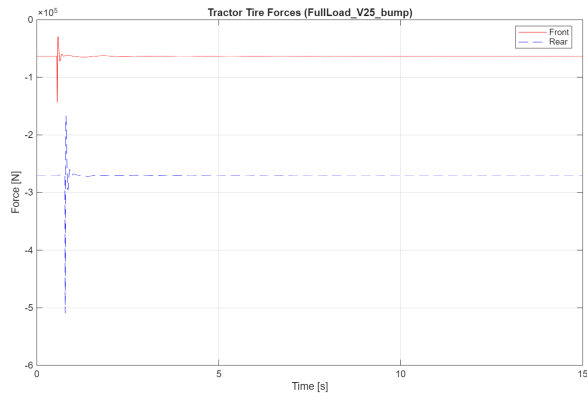


(a) Tractor,  $V = 20$  m/s

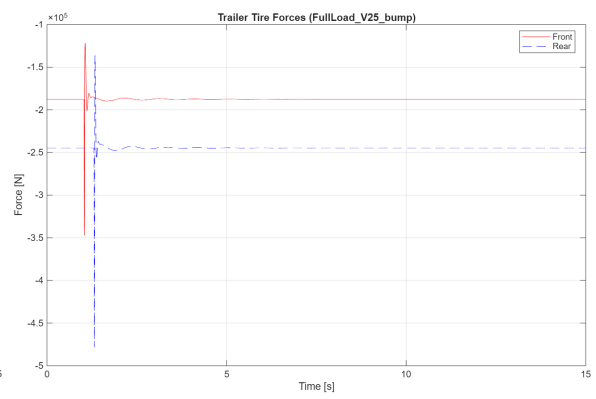


(b) Trailer,  $V = 20$  m/s

Figure 24: Tire contact forces for the FullLoad configuration over the bump profile at  $V = 20$  m/s.



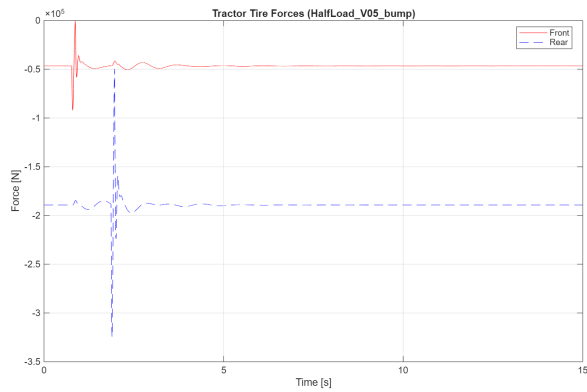
(a) Tractor,  $V = 25$  m/s



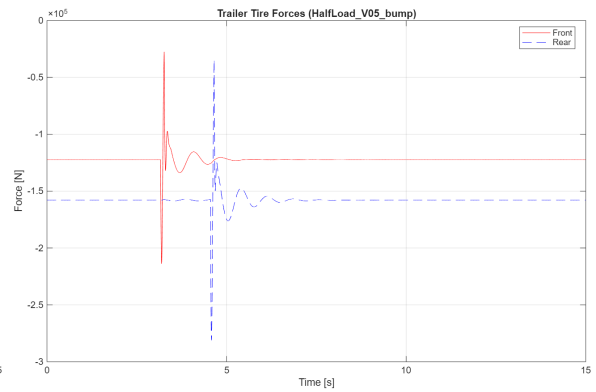
(b) Trailer,  $V = 25$  m/s

Figure 25: Tire contact forces for the FullLoad configuration over the bump profile at  $V = 25$  m/s.

### Half load

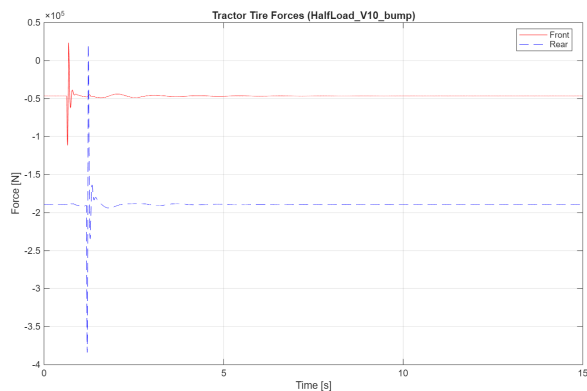


(a) Tractor,  $V = 5$  m/s

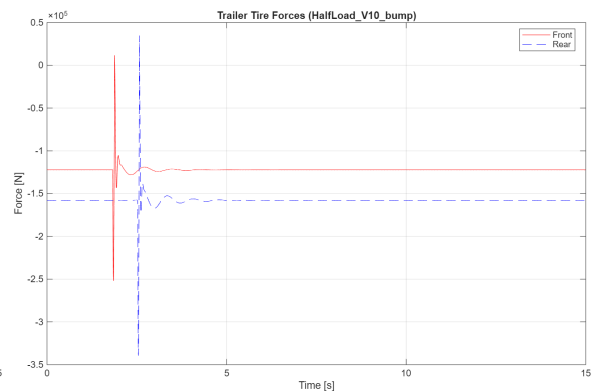


(b) Trailer,  $V = 5$  m/s

Figure 26: Tire contact forces for the HalfLoad configuration over the bump profile at  $V = 5$  m/s.



(a) Tractor,  $V = 10$  m/s



(b) Trailer,  $V = 10$  m/s

Figure 27: Tire contact forces for the HalfLoad configuration over the bump profile at  $V = 10$  m/s.

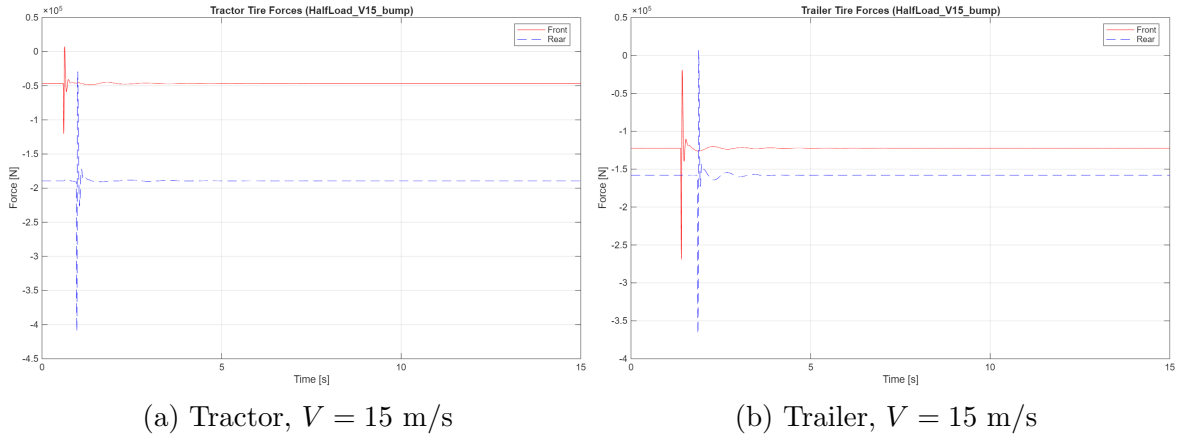


Figure 28: Tire contact forces for the HalfLoad configuration over the bump profile at  $V = 15$  m/s.

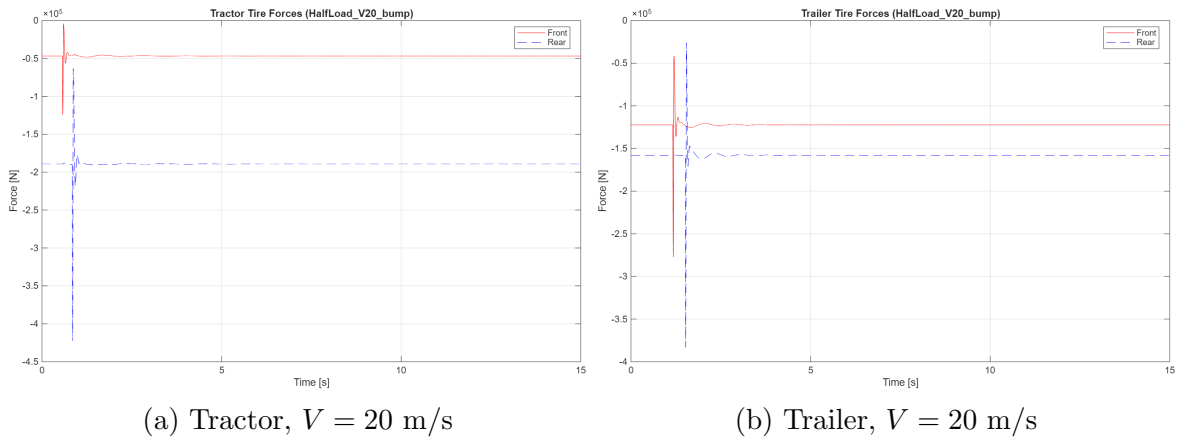


Figure 29: Tire contact forces for the HalfLoad configuration over the bump profile at  $V = 20$  m/s.

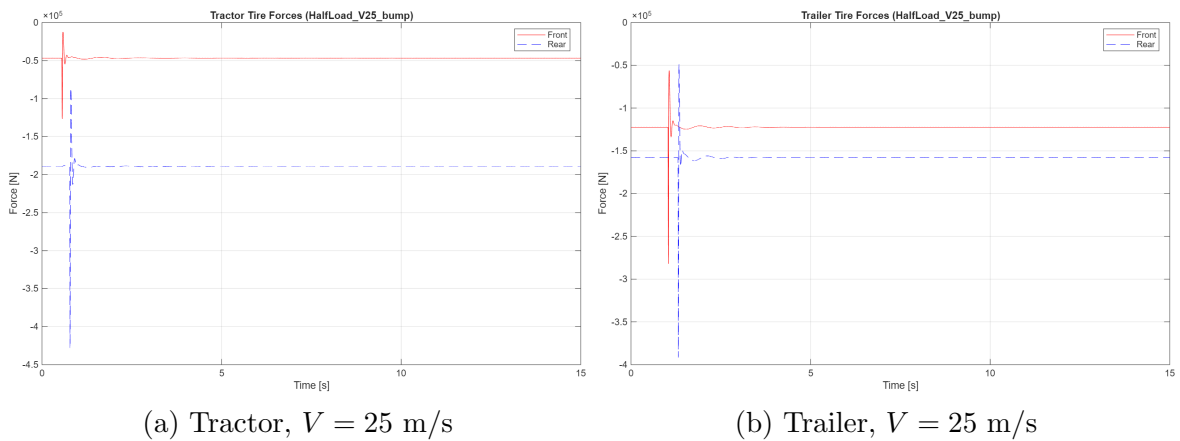


Figure 30: Tire contact forces for the HalfLoad configuration over the bump profile at  $V = 25$  m/s.

## No load

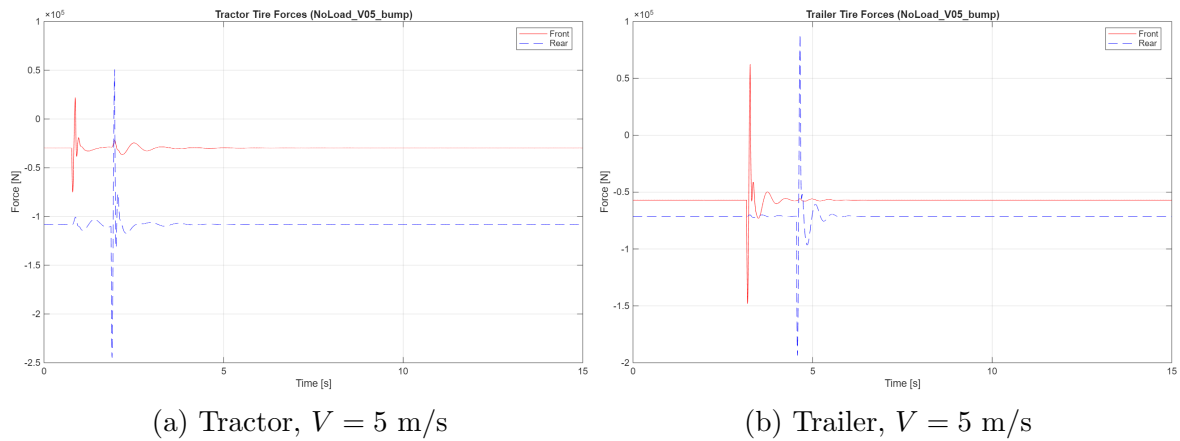


Figure 31: Tire contact forces for the NoLoad configuration over the bump profile at  $V = 5$  m/s.

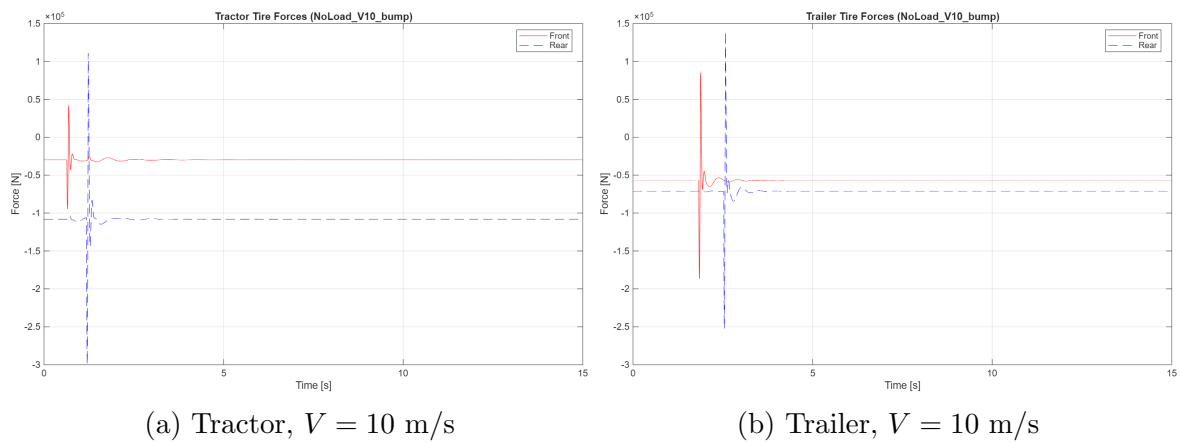


Figure 32: Tire contact forces for the NoLoad configuration over the bump profile at  $V = 10$  m/s.

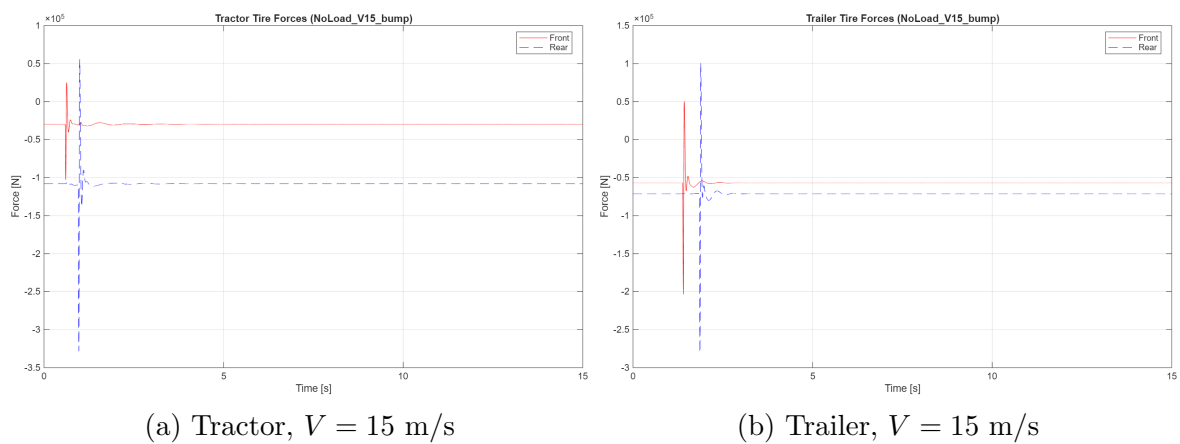
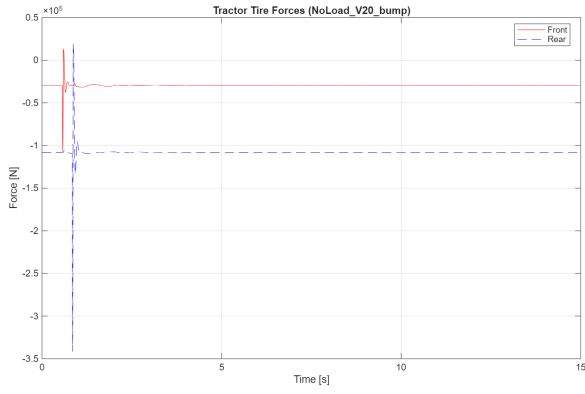
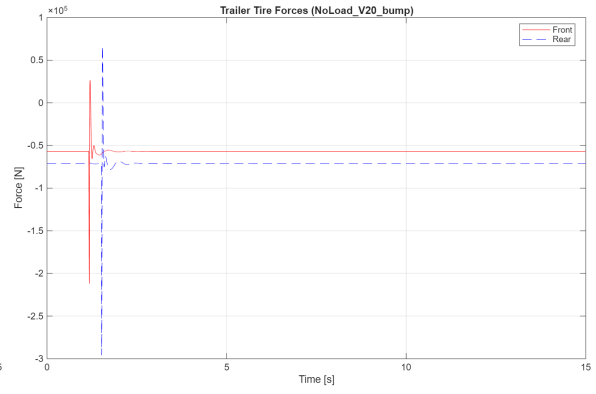


Figure 33: Tire contact forces for the NoLoad configuration over the bump profile at  $V = 15$  m/s.

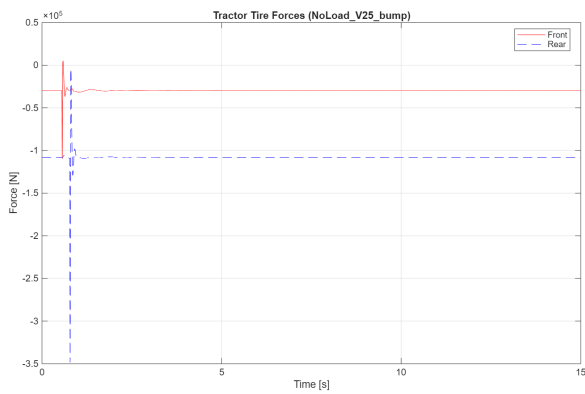


(a) Tractor,  $V = 20$  m/s

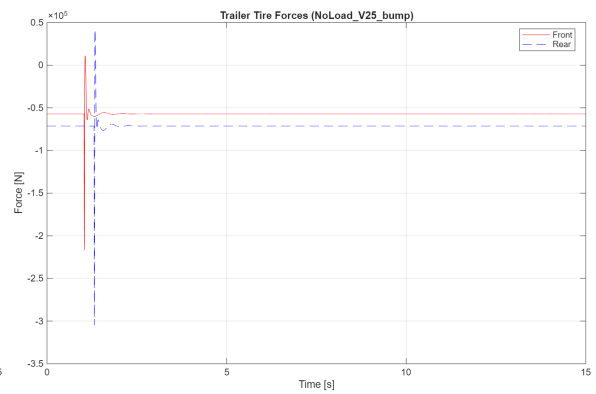


(b) Trailer,  $V = 20$  m/s

Figure 34: Tire contact forces for the NoLoad configuration over the bump profile at  $V = 20$  m/s.



(a) Tractor,  $V = 25$  m/s



(b) Trailer,  $V = 25$  m/s

Figure 35: Tire contact forces for the NoLoad configuration over the bump profile at  $V = 25$  m/s.

## D.2 CASE – 2: Road & Bridge Expansion Joint

To model the road–bridge joint, a step profile was used with a step height of 0.03 m (30 mm), occurring at 1 second. This profile is not dependent on the Vehicle’s Longitudinal Velocity ( $V_x$ ). The choice of a 30 mm step is consistent with Eurocode traffic load modelling guidance, which considers local irregularities for short spans (below 15 m) as being represented by a *30 mm thick plank* (CEN, 1994).

Table 4: Dimensions and timing of the road–bridge expansion joint

Parameter	Value
Step height	0.03 m
Step time	1.0 s
Velocity dependency	Not a function of $V_x$

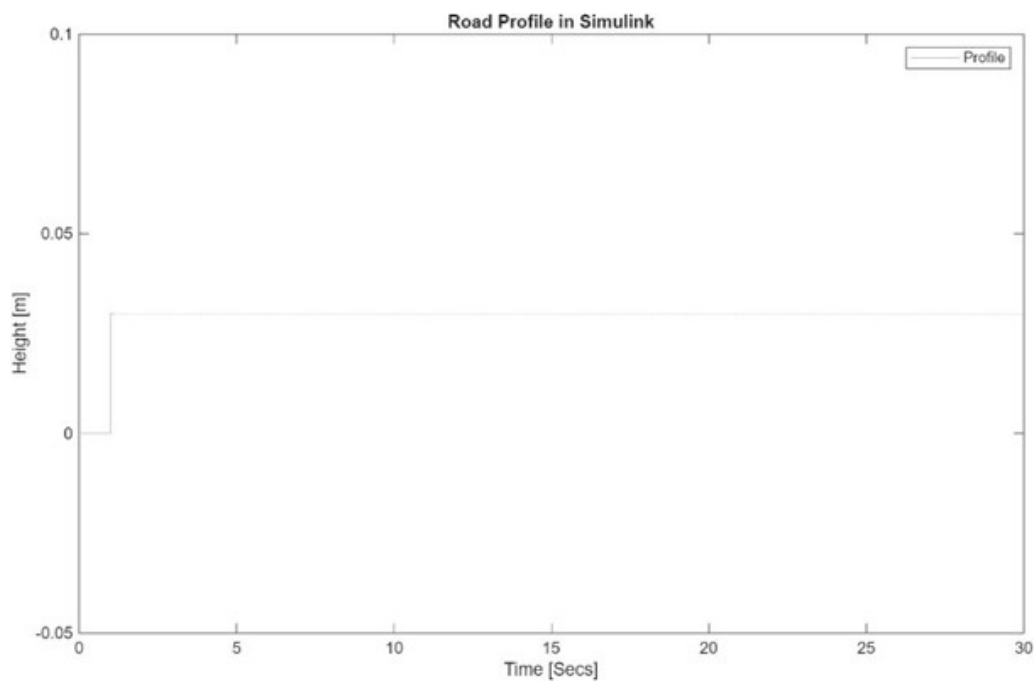
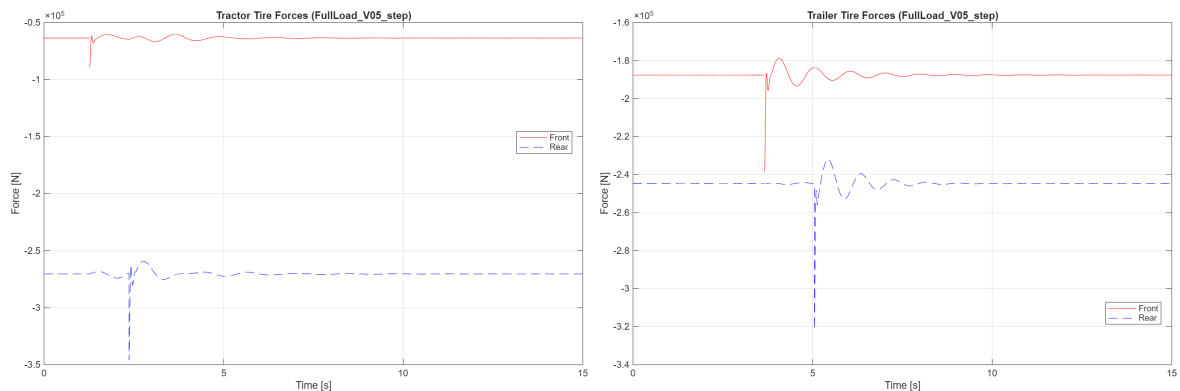


Figure 36: Road–Bridge Expansion Joint Profile

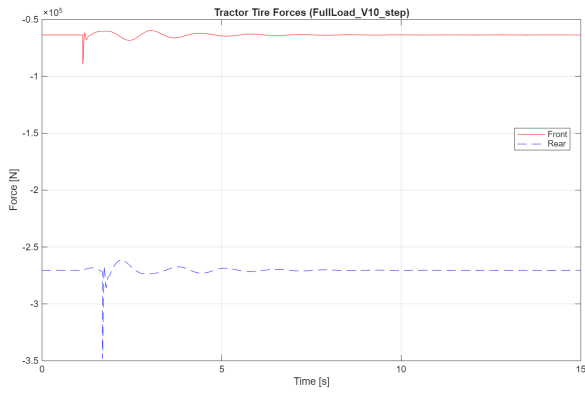
### Full load



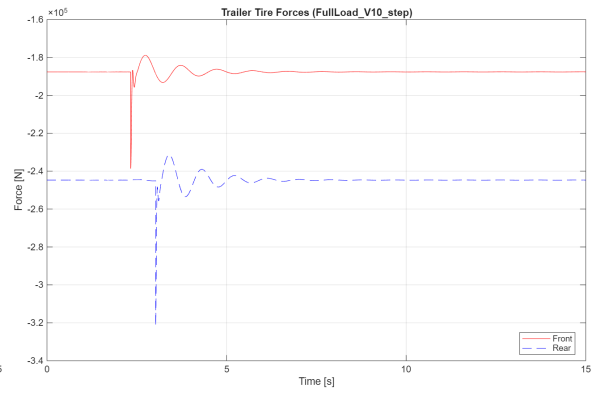
(a) Tractor,  $V = 5$  m/s

(b) Trailer,  $V = 5$  m/s

Figure 37: Tire contact forces for the FullLoad configuration over the step profile at  $V = 5$  m/s.

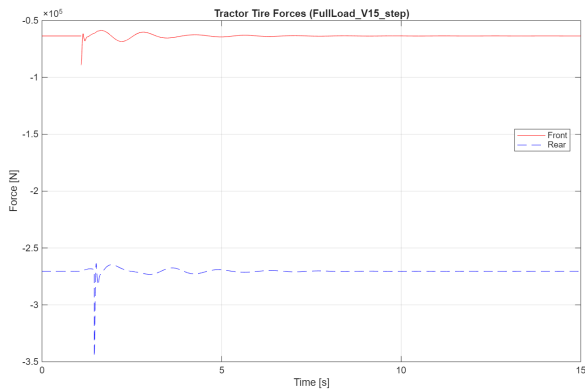


(a) Tractor,  $V = 10$  m/s

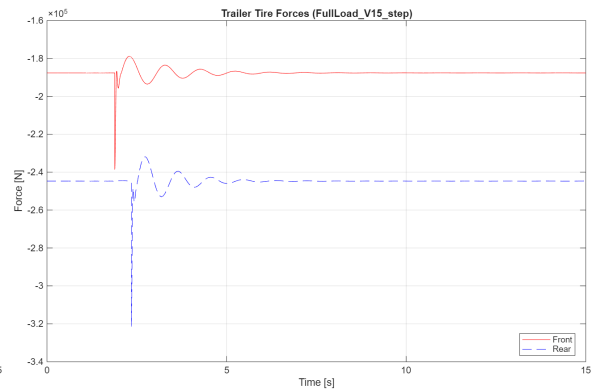


(b) Trailer,  $V = 10$  m/s

Figure 38: Tire contact forces for the FullLoad configuration over the step profile at  $V = 10$  m/s.

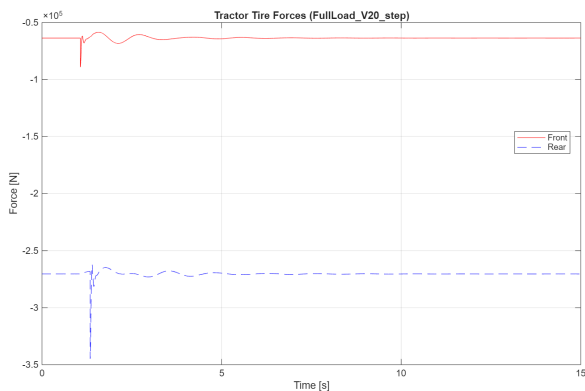


(a) Tractor,  $V = 15$  m/s

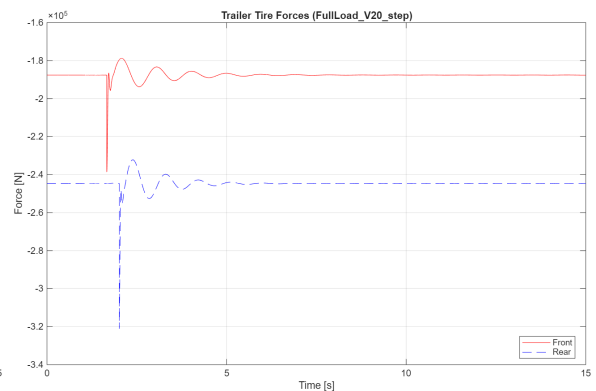


(b) Trailer,  $V = 15$  m/s

Figure 39: Tire contact forces for the FullLoad configuration over the step profile at  $V = 15$  m/s.

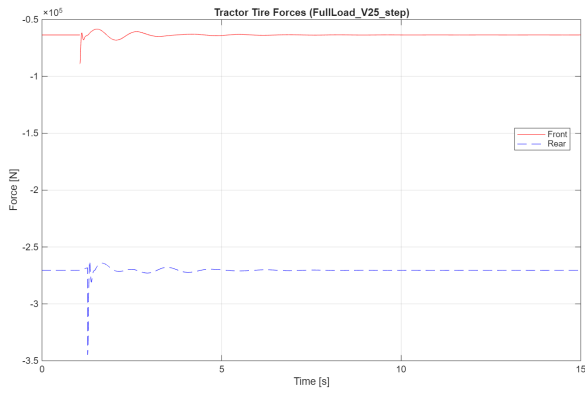


(a) Tractor,  $V = 20$  m/s

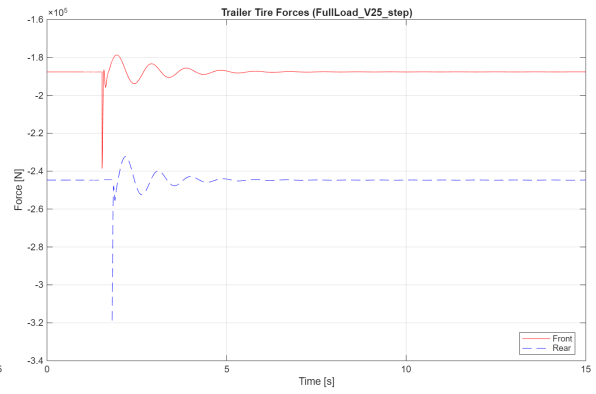


(b) Trailer,  $V = 20$  m/s

Figure 40: Tire contact forces for the FullLoad configuration over the step profile at  $V = 20$  m/s.



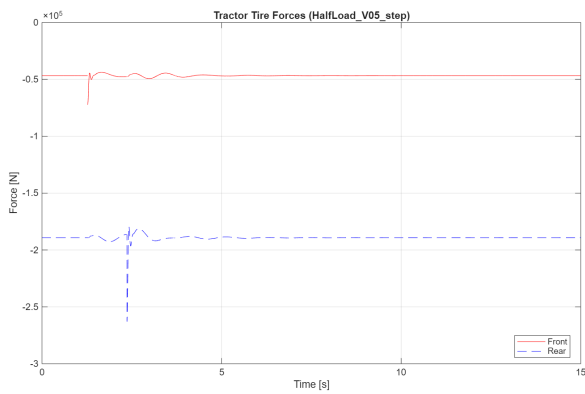
(a) Tractor,  $V = 25$  m/s



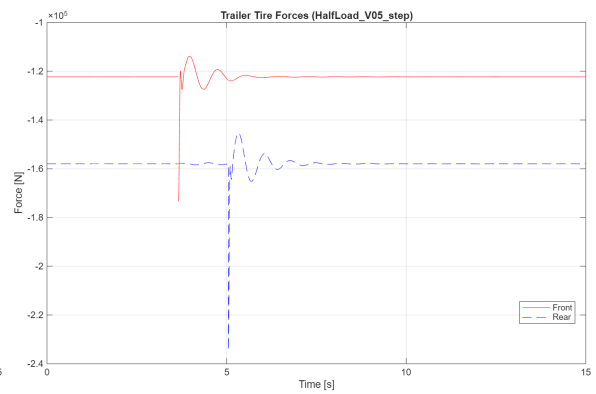
(b) Trailer,  $V = 25$  m/s

Figure 41: Tire contact forces for the FullLoad configuration over the step profile at  $V = 25$  m/s.

### Half load

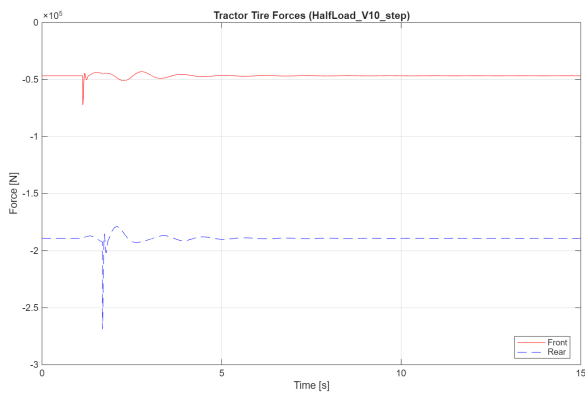


(a) Tractor,  $V = 5$  m/s

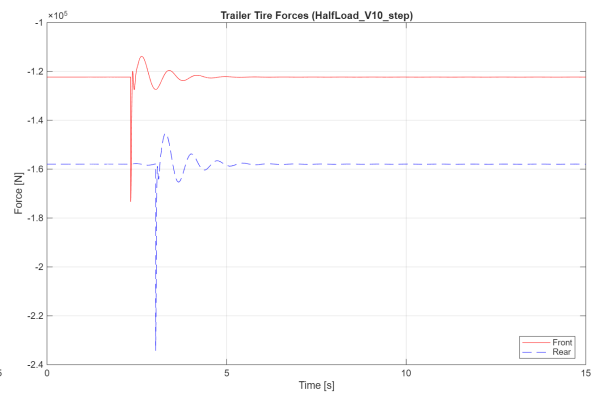


(b) Trailer,  $V = 5$  m/s

Figure 42: Tire contact forces for the HalfLoad configuration over the step profile at  $V = 5$  m/s.

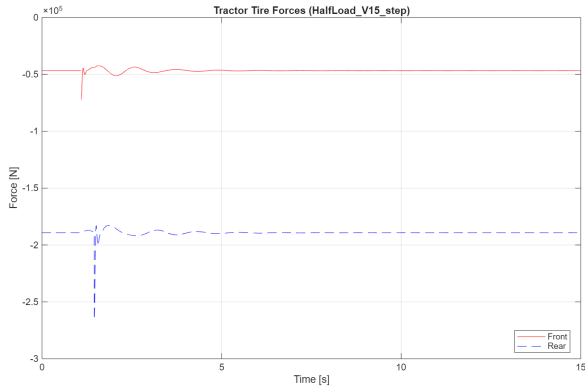


(a) Tractor,  $V = 10$  m/s

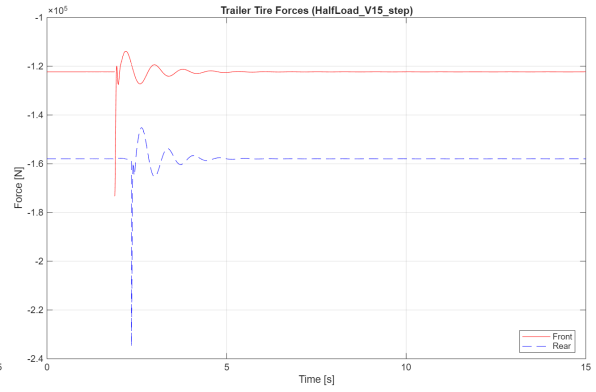


(b) Trailer,  $V = 10$  m/s

Figure 43: Tire contact forces for the HalfLoad configuration over the step profile at  $V = 10$  m/s.

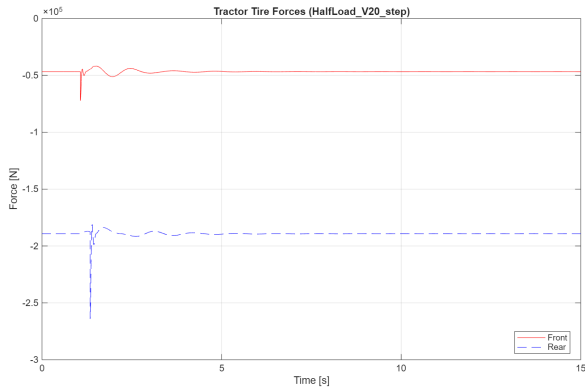


(a) Tractor,  $V = 15$  m/s

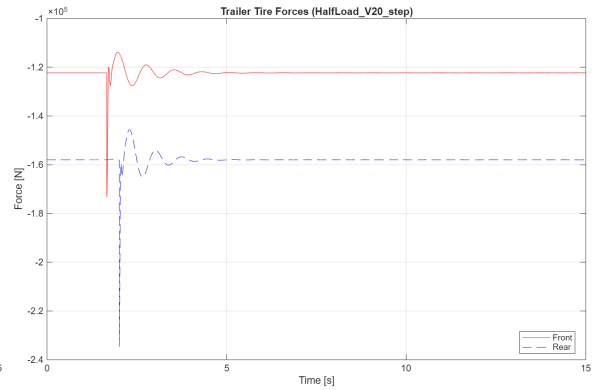


(b) Trailer,  $V = 15$  m/s

Figure 44: Tire contact forces for the HalfLoad configuration over the step profile at  $V = 15$  m/s.

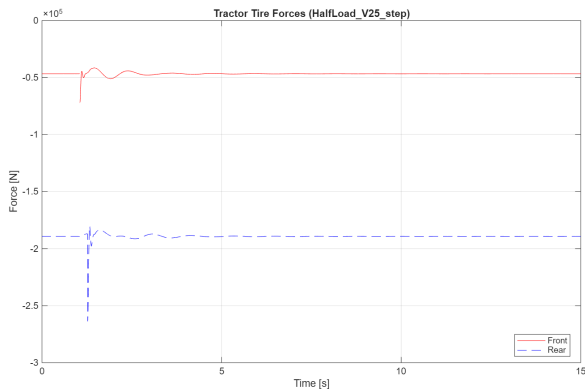


(a) Tractor,  $V = 20$  m/s

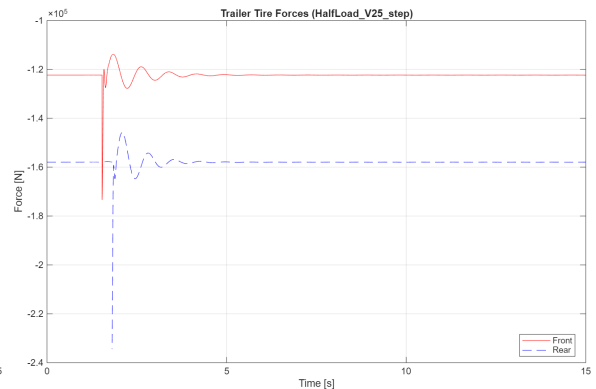


(b) Trailer,  $V = 20$  m/s

Figure 45: Tire contact forces for the HalfLoad configuration over the step profile at  $V = 20$  m/s.



(a) Tractor,  $V = 25$  m/s



(b) Trailer,  $V = 25$  m/s

Figure 46: Tire contact forces for the HalfLoad configuration over the step profile at  $V = 25$  m/s.

## No load

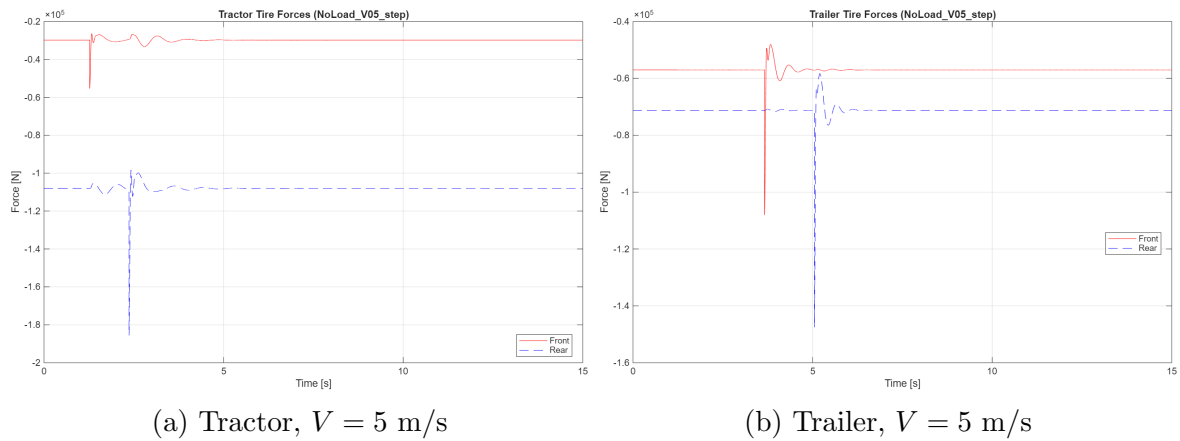


Figure 47: Tire contact forces for the NoLoad configuration over the step profile at  $V = 5$  m/s.

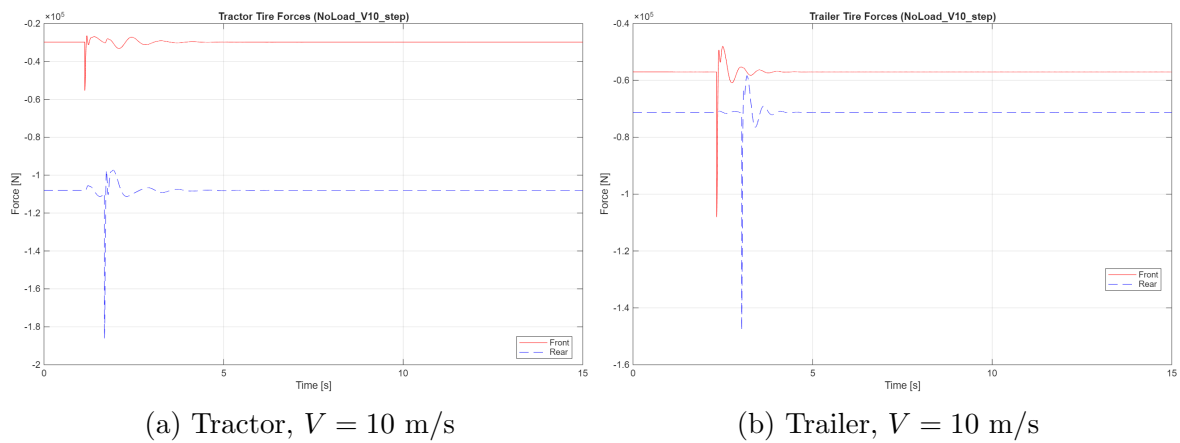


Figure 48: Tire contact forces for the NoLoad configuration over the step profile at  $V = 10$  m/s.

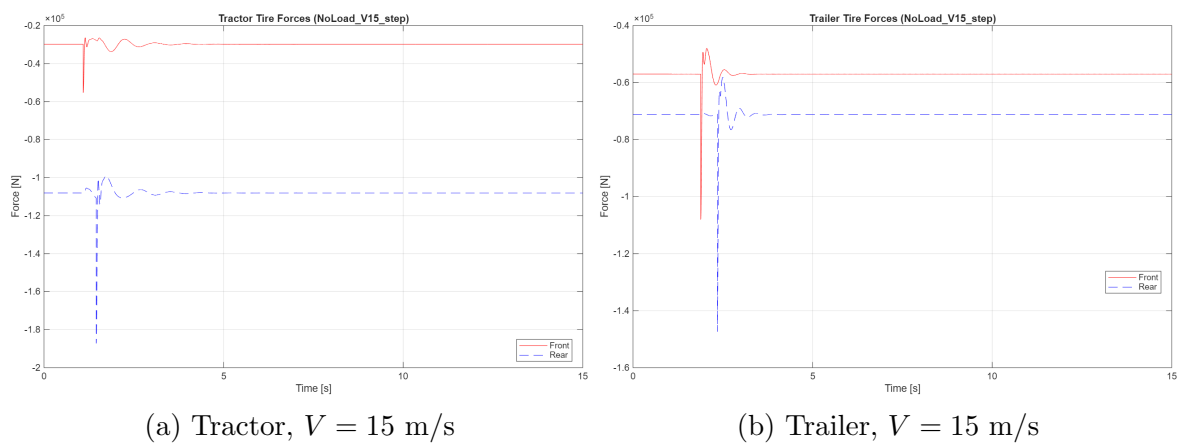
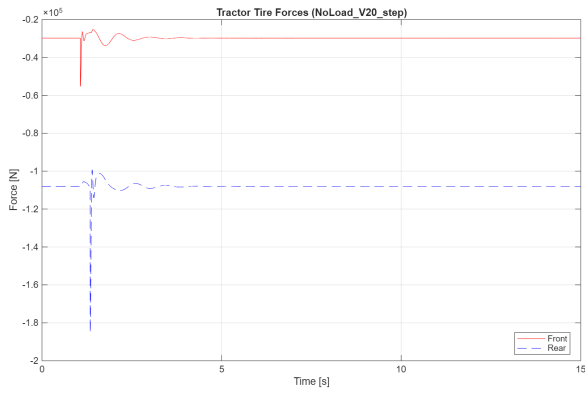
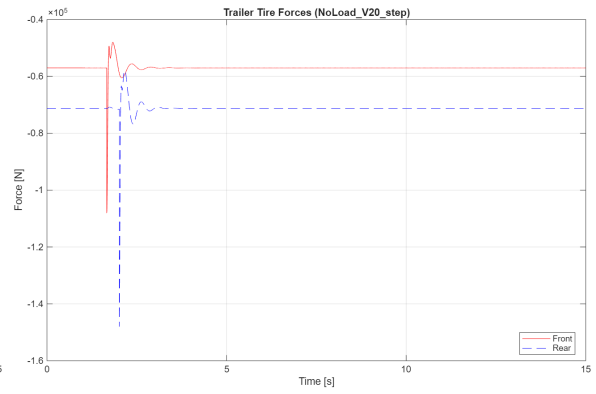


Figure 49: Tire contact forces for the NoLoad configuration over the step profile at  $V = 15$  m/s.

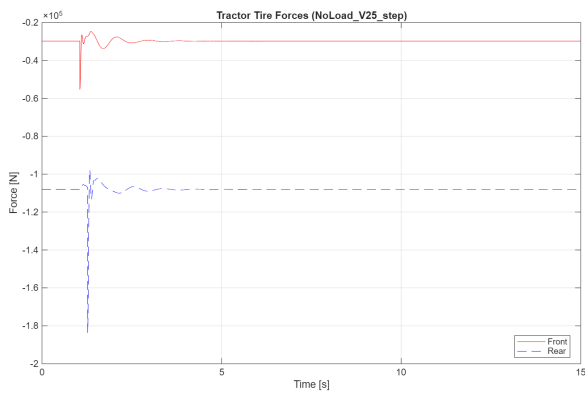


(a) Tractor,  $V = 20$  m/s

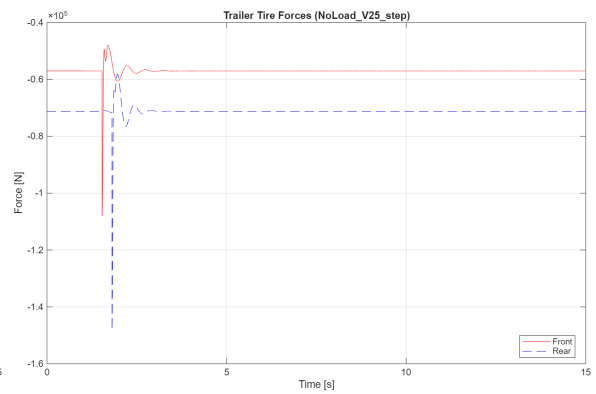


(b) Trailer,  $V = 20$  m/s

Figure 50: Tire contact forces for the NoLoad configuration over the step profile at  $V = 20$  m/s.



(a) Tractor,  $V = 25$  m/s



(b) Trailer,  $V = 25$  m/s

Figure 51: Tire contact forces for the NoLoad configuration over the step profile at  $V = 25$  m/s.